HOST UNIVERSITY: The University of Edinburgh

FACULTY: College of Science & Engineering

DEPARTMENT: School of Engineering

Academic Year 2022-2023

Smouldering of Encapsulated Timber – Effect of Exposure Heat Flux and Encapsulation Material

Rhys Main

Promoter: Dr Rory Hadden

Master thesis submitted in the Erasmus+ Study Programme

International Master of Science in Fire Safety Engineering

Declaration

This master's dissertation is submitted in partial fulfilment of the requirements for the degree of The International Master of Science in Fire Safety Engineering (IMFSE). This master's dissertation has never been submitted for any degree or examination to any other University/programme. The author(s) declare(s) that this master's dissertation is original work except where stated. This declaration constitutes an assertion that full and accurate references and citations have been included for all material, directly included and indirectly contributing to the master's dissertation. The author(s) gives (give) permission to make this master's dissertation available for consultation and to copy parts of this master's dissertation for personal use. In the case of any other use, the limitations of the copyright have to be respected, in particular with regard to the obligation to state expressly the source when quoting results from this master's dissertation. The master's dissertation supervisor must be informed when data or results are used.

This thesis was conducted under the supervision of Dr Rory Hadden.

Abstract

To protect structural timber from the effects of fire encapsulation is commonly adopted, which involves cladding the timber in non-combustible material. However, several large-scale experimental studies have reported occurrences where structural timber has been seen to continue smouldering for a significant duration of time, post fire extinguishment. However, no insight or discussion is given, as this problem was out with their scope and not expected.

Building on the limited current research into this problem, 17 small scale experiments were conducted utilising a cone calorimeter to establish the effect a variation in exposure heat flux has on 1 layer of plasterboard encapsulation. Also, how varying encapsulation build ups will affect the smouldering dynamics, with mineral wool and multiple layers of plasterboard tested. The samples were exposed to a heat flux for a defined period of time, after which it was removed, to simulate fire extinguishment. The mass and combustion gases were analysed to characterise the smouldering dynamics.

The experimental testing highlighted that, with an increased exposure heat flux, a higher mass loss rate can be expected after heat flux removal. Additionally, that differing encapsulation materials and varying layers of plasterboard all affected the observed smouldering.

All but one sample showed signs of self-sustained smouldering, surpassing the expected outcome, highlighting that observations in previous research are not an isolated occurrence, instead this represents a serious hazard that needs to be further investigated to allow for the safe adoption of structural timber in tall structures.

Acknowledgement

Special thanks to Rory, for the opportunity to work on this thesis and his guidance throughout, keeping me true.

Additionally, the PhD students at Edinburgh, for their patience while I bumbled around the lab. But especially David, Laura and Cameron, for the numerous times helping me fix the cone calorimeter and support.

Thank you to IMFSE board for creating a brilliant course and the sponsorship, which made these last 2 years possible.

And finally, my lovely mother, Julia!

Table of Contents

List of Figures

List of Tables

Abbreviations

CO_2	Carbon dioxide
CO	Carbon monoxide
CLT	Cross laminated timber
HRR	Heat release rate
HRRPUA	Heat release rate per unit area
MLR	Mass loss rate
O_2	Oxygen

1 Introduction

Due to observed climate change caused by greenhouse gas emissions, and society's growing interest in sustainability, the construction industry has undergone significant transformations, highlighting the need for environmentally conscious design and material selection.

The development and adoption of engineered timber products, with new construction methods has been accelerated worldwide in recent decades as a result of this mental shift because of its desirable environmental benefits. Firstly, compared to steel and concrete, timber has a very low embodied energy (Committee on Climate Change, 2019). Secondly, it is a renewable material with many countries implementing sustainable forestry management. Thirdly, it has the potential to act as a carbon sink, absorbing more CO_2 than is produced for its manufacturing (Ramage et al., 2017).

Timber has commonly been utilised for small-scale, low-rise structures throughout Northern Europe and North America in the form of timber frame construction. The main change is coming within medium to high rise structures, which has seen a significant uptake in the adoption of engineered timber products, specifically CLT. The first predominantly timber high rise to gain recognition was Stadthaus in London (Karacabeyli and Lum, 2022). Since then, the boundaries have continuously been pushed, with structures up to 17 stories tall and feasibility proposals/designs for structures up to 80 stories tall (Foster et al., 2017).

This rapid advance can be seen as a major triumph within the industry, however, due to the swift uptake there are still many areas of insufficient knowledge with ongoing research, especially the fire behaviour of tall timber structures (Östman et al., 2017). This lack in fire behaviour knowledge is compounded by the fact that, historically, timber has been forbidden for larger structures, with non-combustible materials adopted in-lieu (Östman et al., 2017), brought about by building regulations adopting prescriptive methods for fire safety. However, as we shift to performance-based design, giving designers greater flexibility and creative freedom, we are seeing the maximum height of timber structures increasing, with tall timber buildings continuously being constructed.

With an increase in building height, the associated risks and fire safety requirements increase too. Evacuation times of high-rise buildings are substantially greater, requiring longer protection times. Furthermore, an increase in building storeys increases the possibility for situations where complete evacuation is not possible, with ‘stay-put’ strategies adopted (Buchanan et al., 2014) (Östman et al., 2017) or scenarios where the fire floor blocks egress for the floors above.

To help mitigate these risks and ensure life safety of the occupants, limiting fire spread and preventing structural collapse is paramount. This can result in lengthy protection times and, subsequently, fire

resistance designs for complete burnout are adopted. To achieve this, the utilisation of passive and active fire protection is paramount, with the most commonly adopted measures being sprinklers and timber encapsulation.

Encapsulation of timber involves cladding the timber element in a non-combustible material, protecting the combustible timber from the effects of the fire. Encapsulation materials tend to have a low thermal conductivity and diffusivity, delaying the time at which heat is transferred to the timber, resulting in longer ignition times. This inherently increases the fire resistance of the member (Ranger et al., 2020). Additionally, encapsulation helps limit the contribution of the timber element to the fire. Typical encapsulation materials are gypsum plasterboard, mineral wool insulation and cement screed for flooring.

Buchanan (Buchanan et al., 2014) purposed a performance criterion for timber structures, with the level of encapsulation increasing with height, with full encapsulation recommended for tall timber structures. When fully encapsulated, timber is said to have the same fire resistance of a non-combustible material.

Table 1: Encapsulation performance criteria for variation in building height (adopted from (Buchanan et al., 2014))

Building height	**Possible level of specified performance**	**Possible design strategy for timber elements**
Low-rise buildings	Escape of occupants with no assistance. No property protection	**No encapsulation**
Mid-rise buildings	Escape of occupants with no assistance. Some property protection	**No encapsulation**
Taller buildings	Escape with firefighter assistance. Burnout with some firefighter intervention	**Limited encapsulation**
Very tall buildings	Protect occupants in place. Complete burnout with no intervention	**Full encapsulation**

1.1 Problem Description

Due to the nature of encapsulating materials, they are good thermal insulators due to their low thermal conductivity. However, if exposed for long enough, the protected timber will begin to smoulder. Herein lies the issue. If the protected timber begins to smoulder before fire extinguishment, the encapsulating material will help reduce the heat losses from the timber, fostering conditions that are prime to sustain smouldering. Generally, timber requires an external heat source to sustain burning, with self-extinguishment observed at heat fluxes below 6kW/m^2 (Crielaard et al., 2019).

However, the effect due to the presence of encapsulation is not fully understood when concerned with self-extinguishment of the underlying timber.

There has been a handful of research projects that have observed self-sustained smouldering post fire extinguishment (Wiesner et al., 2021) (Su et al., 2018a) (Kotsovinos et al., 2023). All these projects were large scale experiments, with smouldering observed from different experimental arrangements.

Wiesner (Wiesner et al., 2021), reported unexposed CLT ceiling slabs that structurally collapsed 29hours post fire extinguishment. This was attributed to self-sustained smouldering deep within the CLT panels. Compartment fire experiments by NFPA (Su et al., 2018a) adopting unexposed CLT, recorded continued smouldering at the joints between adjacent panels with a transition into flaming intermittently observed. Finally, and most recently, during compartment fire experiments with partial encapsulated CLT, smouldering at joints between CLT was observed after 36 hours post fire extinguishment (Kotsovinos et al., 2023). Furthermore, a select number of these smouldering points progressed behind the encapsulating material, encompassing a significant area.

Adoption of encapsulation for passive fire protection is widely adopted within industry, utilised to achieve certain fire resistance period. However, the specification of fire resistance does not account for the cooling stage of the fire. If situations arise where smouldering is able to progress and sustain itself behind encapsulation post fire extinguishment, the timber members could slowly lose mass and reduction in its structural capacity, until failure.

Therefore, being able to identify situations where sustained smouldering can occur and which conditions are paramount is of the utmost importance in providing safe designs incorporating encapsulated timber.

Current encapsulation research is predominantly focused on the time delay of timber charring from when exposed to fire and the thermal response of the encapsulating material, omitting discussions and research into sustained smouldering post exposure. This has been highlighted as a serious hazard within numerous industry reports (Ronquillo et al., 2021) (Bartlett et al., n.d.) stating that further research is required for self-sustained smouldering of encapsulated timber to help facilitate more widespread adoption within the construction industry, giving regulatory bodies and designers greater confidence.

1.2 Aims and Objectives

This report will look to investigate the conditions for self-sustained smouldering of encapsulated timber post exposure to a fire. It will lead on from previous research completed at the University of

Edinburgh (Li, 2022), with added emphasis on practices used within industry, plasterboard type encapsulation, with samples arranged vertically to replicate walled construction.

The research will look to investigate the effects varying exposure heat fluxes and encapsulation materials will have on the smouldering dynamics, particularly the MLR.

Therefore, the following objectives have been set:

- Review of current research for smouldering of encapsulated timber and situations where it has occurred, to guide experimental set up and sample conditions.
- Small scale testing of samples.
- Quantify and analyse the effect a variation in heat flux and encapsulation materials has on the smouldering dynamics.
- Analyse whether the tested conditions created a positive environment for self-sustained smouldering.

2 Literature Review

2.1 What Is Smouldering?

Despite its well documented and researched characteristics, the field's current understanding of smouldering combustion for timber is lacking, due to a combination of the complexity and coupling of thermochemical and transport process within a reactive porous fuel (Rein, 2016). This is a cause for concern within the built environment, as smouldering poses a major hazard, due mainly to its high yield of toxic gases and possible pathway to flaming combustion (Rein, 2016). From a structural engineering standpoint, burning of timber results in loss of mass, reduction of member sizes and a reduction of its mechanical properties (Wiesner, 2019), resulting in reduced structural capacity leading to the possibility of a structural failure/collapse. It has been found that smouldering and flaming combustion result in comparable mass loss rate, indicating that sustained smouldering poses a major threat and is damaging to the structural capacity (Richter et al., 2021).

In layman terms, when a solid fuel source is involved with combustion the overall reaction can be summarised by two processes, pyrolysis which is followed by oxidation (Ohlemiller, 1985) (Rein, 2016). Pyrolysis is the chemical decomposition of the fuel brought about by increased thermal energy (heating). It is an endothermic reaction, resulting in gaseous products, pyrolysate and solid products, char. Oxidation is an exothermic chemical reaction that occurs when these products come into contact with oxygen, normally found within air.

The location of the oxidation reaction determines what type of combustion shall be dominant: flaming or smouldering. Flaming combustion occurs when the pyrolysate gases surrounding the fuel are oxidised, while smouldering combustion occurs when the solid char on the fuel surface is oxidised (Ohlemiller, 1985) (Rein, 2009). This results in flameless combustion, with certain fuels experiencing a glowing colour (Rein, 2013).

The pyrolysis and oxidation reactions are summarised below:

Pyrolysis:

$$Fuel\ (solid) + Heat \rightarrow Pyrolysate\ (gas) + Char\ (solid) + Ash\ (solid) \quad (1)$$

Heterogeneous oxidation:

$$Char\ (solid) + O_2\ (gas) \rightarrow Heat + CO_2 + H_2O + Other\ gases + Ash\ (solid) \quad (2)$$

Gas-phase oxidation:

$$Pyrolysate\ (gas) + O_2\ (gas) \rightarrow Heat + CO_2 + H_2O + Other\ gases \quad (3)$$

Apart from the location of the oxidation reaction, smouldering and flaming combustion differ greatly. As mentioned, smouldering is flameless, resulting in low peak temperatures, normally within the range of 450-700°C (Rein, 2009), compared to 1400-1800°C for flaming (Drysdale, 2011). This corresponds to a lower effective heat of combustion, with typical values of 6-12kJ/g, compared to 16-30kJ/g (Rein, 2016). The heat release rate per unit area (HRRPUA) for flaming combustion depends greatly on the fuel type and environmental conditions, with values upwards of 150kW/m^2 possible for timber. Again, smouldering experiences significantly smaller HRRPUA, with the burning front having typical values of 10-30 kW/m^2 (Ohlemiller, 1985). All these factors contribute to a slow propagation rate, with smouldering fires typically spreading at 1mm/min (Rein, 2016).

By nature, smouldering is an incomplete oxidation process, due to its low temperature (Rein, 2016), resulting in higher yields of toxic gases, particularly CO. A CO to CO_2 ratio of 0.6 to 1 is common for smouldering fuels, drastically lower than that for flaming combustion, where the ratio is 10 (Rein, 2009) (Purser, 2002).

A large array of fuels can sustain smouldering, however, they all have comparable properties. The physical composition requires a permeable medium, normally formed from grains, fibres or other porous structures. This creates a large surface area per unit volume for the oxidation reaction and facilitates the oxygen transport through the fuel bed (Ohlemiller, 1985) (Rein, 2009). These fuels form char on heating, which insulates the reaction zone, reducing the heat losses to the environment (Ohlemiller, 1985).

2.1.1 Smouldering Propagation

Smouldering propagation is dominantly controlled by two factors, oxygen supply and heat losses (Ohlemiller, 1985) (Rein, 2013). A steady supply of oxygen is required for diffusion at the reaction zone to allow the oxidation reaction. It has been found from previous experimental work that the oxygen concentration plays a critical factor in the type of burning behaviour experienced, with smouldering occurring between 4-15% (Richter et al., 2021), highlighting the lower oxygen concentration requirement for smouldering combustion compared with that required for flaming combustion, normally taken as 16% (Drysdale, 2011). Additionally, testing completed in varying concentrations of O_2 have established that the pyrolysis reaction contributes the majority of MLR (Richter et al., 2021) (Morrisset et al., 2021). In addition, the airflow speed over the reaction surface has an impact (Crielaard et al., 2019).

Heat loss plays another crucial role in the process. The heat produced from the exothermic oxidation reaction is required to pyrolyse the fresh fuel. Therefore, if the heat losses to the environment are too great the system does not have enough energy to lead to pyrolysis.

2.1.2 Timber Smouldering

Timber compromises of three natural polymers, cellulose, hemicellulose and lignin, which are interconnected to form a cell structure (Ramage et al., 2017). These cells are arranged longitudinally, creating porous fibres and forming timber's grain. Due to this, timber is an anisotropic material, meaning its properties change with grain direction.

In terms of burning, the grain direction has direct impact on multiple properties, however, in terms of smouldering, two in particular. The permeability of timber changes with grain direction, with permeability along the grain being four orders of magnitude higher (Friquin, 2011). This allows for significantly greater oxygen transport through the timber, to the oxidation reaction zone. While also allowing for greater flow volatile gases produced from pyrolysis, aiding heat transfer (Bartlett et al., 2019). The grain direction also influences the moisture movement during the heating of timber. Finally, the thermal conductivity of timber is greater parallel to the grain, thus, helping with heat transfer deeper into the timber. These factors result in the charring rates typically higher parallel to the grain. Bartlet et al. (Bartlett et al., 2019) provides a comprehensive review of experimental research into these properties and the other dominating factors.

2.1.3 Propagating Timber Smouldering Front

The structure of a smouldering front in timber can be split into 4 distinct zones, highlighted on Figure 1 and explained below:

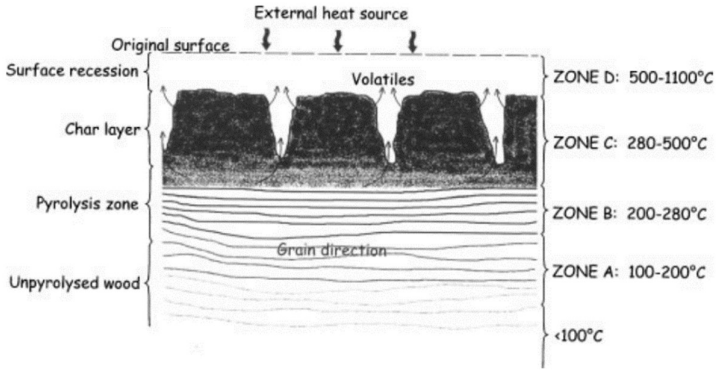

Figure 1: Smouldering front in timber (taken from (Friquin, 2011))

<u><100°C</u>

Permanent reduction in timber's strength occurs. The extend of this depends on numerous factors, such as moisture content, exposure period, and heating regime. This has been found to be around >65°C (Dietenberger and Hasburgh, 2016)

Zone A - 100-200°C

Within this temperature range, the dehydration process of the timber occurs. The free unbound moisture evaporates producing water vapour. From 160-200^{O}C, the organic polymers, cellulose, hemicellulose and lignin start to decompose and with a very slow rate of pyrolysis. Gases emitted in this range are non-combustible.

Zone B – 200-280°C

The pyrolysis of the timber is still relatively slow. The emitted gases are largely non-combustible, however above 225°C, these can be ignited with aid of piloted ignition.

Zone C – 280-500°C

Major changes in the cellular structure start to occur and by 300°C char is rapidly forming, indicating a high rate of pyrolysis. Combustible gases are being emitted,

Zone D - >500°C

By this point the production of volatiles gases is complete. The char will continue to smoulder and oxidise.

The zones and temperature ranges described above is only one model used to describe a smouldering front (Friquin, 2011). Other models published (White and Dietenberger, 2010) follow the same regions, but with a slight differences in the temperature ranges of 25-50°C.

The burning rate of timber can be summarised by equation 4:

$$\dot{m}'' = \frac{\dot{Q}_F'' - \dot{Q}_L''}{L_v} \quad (4)$$

Where, Q_F equals the heat flux from the flame or oxidation reaction to the fuel surface, Q_L is heat losses and L_V is heat of gasification. From this equation it can be seen that in order for sustained smouldering to be supported, $Q_F > Q_S$. Research has shown that in reality, generally $Q_L > Q_F$ for slabs of timber, leading to non-sustained combustion (Drysdale, 2011). Therefore, in order to induce sustained burning, an external heat flux is required, Q_E, such that $Q_F + Q_E > Q_L$. Hence, equation 1 can be re-written as:

$$\dot{m}'' = \frac{\dot{Q}_F'' + Q_E'' - \dot{Q}_L''}{L_v} \quad (5)$$

This is commonly observed when burning single pieces of timber (Drysdale, 2011), which are unable to sustain combustion without an external heat flux.

2.2 Theory for Smouldering of Encapsulated Timber

Encapsulation materials are designed to prolong the time before the timber is involved within the fire (delay of ignition and combustion of the encapsulated timber) (Ranger et al., 2020), hence they tend to have extremely good thermal insulation properties minimizing the heat transfer. However, if subjected to long exposure times and/or extreme heat fluxes, enough energy will be conducted through the material, leading to the pyrolysis and ignition of the timber. Herein lies the problem.

Once the initial fire is extinguished, no more heat can be transferred into the system, meaning that Q_E is zero. Heat from the smouldering front is partially conducted to the fuel bed to advance the pyrolysis front, Q_F, with the remaining heat lost in the environment and surroundings, Q_L. As discussed prior, without the external heat flux, $Q_L > Q_F$ resulting in non-sustained smouldering. But due to the encapsulating material insulating properties, Q_L is significantly reduced, as the heat can't easily be lost from the surface due to conduction and convection. This can create conditions where $Q_F > Q_L$, resulting in self-sustained smouldering.

The other dominant characteristic that affects smouldering is the oxygen supply to the reaction zone. This supply would be impeded by the presence of an encapsulation material, with the extent dependent on the adopted encapsulating material. For example, due to its fibrous structure, mineral wool insulation would allow for greater oxygen transfer than plasterboard.

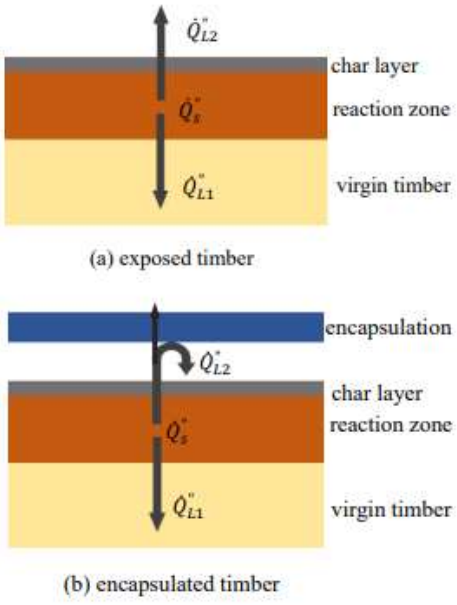

Figure 2: Diagram of heat transfer in exposed and encapsulated timber (Taken from (Li, 2022))

2.2.1 Where Has Self-Sustained Smoulder Been Observed

Wiesner et al., (Wiesner et al., 2021), evaluated the structural response of exposed CLT panels when subjected to varying heating conditions from below. Two large-scale CLT slabs were tested in a furnace, with an additional 3 compartment fire experiments utilising CLT slabs for the ceilings. The slabs were subjected to a standardised loading, in line with prescribed accidental loading conditions. One of the compartment experiments experienced structural collapse 29 hours after the start of the heating, well beyond the compartment burnout. This was attributed to unobserved self-sustained smouldering, however, this observation fell out with the scope of the report and no further discussion is given. Additionally, as the samples were exposed CLT panels, no comparison for encapsulation methods can be drawn on.

As part of an extensive multi-phase research project for NFPA, with the goal to quantify the fire load contribution of CLT to an enclosure fire, NIST conducted large-scale compartment fire experiments, adopting exposed CLT for the load bearing structure (Su et al., 2018a). The experimental data showed evidence of continued self-sustained smouldering within certain CLT wall panels post burnout, albeit minimal. These conditions were most prevalent at joints, either panel to panel or panel to ceiling and these sustained deeper charring. Additionally, when prolonged smouldering was observed, a transition into flaming combustion was observed numerous times (Su et al., 2018a).

As the CLT was exposed, there would be substantial heat losses through the surface, leading to unfavourable conditions for self-sustained smouldering. However, at the smouldering joints, the two panels were adjacent with a minimal gap separating, creating a feedback system with radiative heat transferred to the adjoining panel and the possibility for convection depending on the airflow.

This trend was also observed by Kotsovinos (Kotsovinos et al., 2023) during a large scale experiment looking to research the impact that partial encapsulation has on compartment fire dynamics. A compartment, comprising concrete walls and beams supporting CLT ceiling slabs, was exposed to a predefined wood crib fire adopted from previous benchmark experiments. The CLT ceiling was encapsulated with 3 layers of 12.5mm plasterboard over the central portion covering 50% of the area.

From visual inspection and the adoption of thermal imaging cameras, 9 locations of smouldering were observed 12 hours post flame extinguishment within the CLT, with 5 locations observed at 36 hours. These were all observed at the junction between the CLT panels and the walls, promoting radiative feedback. It was noted that no smouldering spots were observed to originate behind the encapsulation. Nevertheless, 2 of the spots progressed under the encapsulation material, covering an area of 1.3x4m and both fully smouldered through the CLT panels, creating holes. This was attributed to reduced heat losses due to the encapsulation. Typically, plasterboard will begin to degrade once

subjected to heating, however, no smouldering was observed directly behind the plasterboard, highlighting its integrity post exposure and, therefore, still providing adequate insulation properties for the smouldering behind.

2.2.2 Research Into Encapsulated Timber

Research into encapsulation has predominantly been into the encapsulation time (time delay until charring onset) for different materials, with variables such as exposure time, heat flux and encapsulation thickness being investigated (Chorlton and Gales, 2020) (Hasburgh, 2016) (Bijloos et al., 2014) (Mitchell et al., 2023) (Su et al., 2018b). As these studies were into the encapsulation time, the majority of them were ceased once charring was observed for the timber being protected, meaning no conclusion could be drawn into conditions for self-sustained smouldering.

2.2.3 Self-Sustained Smouldering Research

To date, minimal research has been published which focuses specifically on conditions that lead to self-sustained smouldering.

Due to the observed self-sustained smouldering within (Su et al., 2018a) and (Wiesner et al., 2021) experiments, (Li, 2022) sought to characterise conditions and factors that could influence its occurrence. Small-scale samples of solid timber were exposed to a 50kW/m^2 radiative heat flux utilising the cone calorimeter, with all samples positioned horizontally. The samples were all 10x10mm and clad in differing encapsulating materials to their front surface, with the sides typically wrapped with an insulating material. Overall, 11 different arrangements were tested, with 3 main variables evaluated - exposure time, encapsulation material and insulation material around the side of the sample.

Three of the experiment set-ups resulted in self-sustained smouldering. All these samples were encapsulated in mineral wool and adopted it for the side insulation, with the only different variable being the exposure time (Li, 2022) The adoption of mineral wool allowed oxygen transfer to the reaction zone, while maintaining minimal heat losses.

When compared to samples with the same encapsulation material, i.e. mineral wool, but adopted aluminium foil or no insulation for the sides, no self-sustained smouldering was achieved. The aluminium foil hindered the oxygen supply to the reaction zone, but also helped limit the heat losses. However, no discussion on the difference in the insulating properties and their effect, was given between the foil and mineral wool. The sample with no side insulation allowed for the greatest oxygen supply to the reaction zone, but the heat losses were too significant to maintain smouldering.

The effect of 4 varying encapsulation arrangements was also assessed. Based on the previous findings, that foil insulation did not lead to smouldering, the 4 samples were insulated with mineral wool. Again, to allow for sufficient oxygen transfer and minimal heat losses.

The tested arrangements were: gypsum plasterboard, 2 layers of gypsum plasterboard, mineral wool and no encapsulation. The sample with no encapsulation adopted an initial layer of mineral wool encapsulation during the exposure time to help induce smouldering, but once the heat flux was removed, so was the mineral wool. Due to this, the specimen encountered major heat losses, resulting in the smouldering being extinguished. As previously mentioned, the mineral wool encapsulation led to self-sustained smouldering.

The plasterboard samples did not lead to self-sustained smouldering. During the heating phase, the samples exhibited similar behaviour to that of the mineral wool, however, once the heat flux was removed, the smouldering swiftly extinguished. This was attributed to plasterboard's changing thermal properties once heated.

When plasterboard is heated, it undergoes dehydration processes, losing water molecules bound within the chemical structure (Ghazi Wakili et al., 2015). This absorbs an extensive amount of energy and is an endothermic reaction by nature (McLaggan et al., 2018). It is this process that helps provides the fire resistance period to the substrata, delaying the transfer of energy and subsequently delaying an increase in temperature. At approximately $600^{O}C$, decarbonation occurs, leading to the decomposition of the boarding (Zehfuß and Sander, 2021). Research has shown that past this phase the thermal conductivity begins to increase, surpassing initial ambient conditions (Ghazi Wakili et al., 2015). This increase in thermal conductivity would lead to greater heat transfer from the sample, resulting in significant heat losses and extinguishment of smouldering.

3 Methodology

To evaluate the conditions for self-sustained smouldering of timber, experimental testing was completed. As described within section 2, smouldering is an inefficient form of combustion, hence when timber smoulders it produces large quantities of combustion products, mainly CO and CO_2. This process consumes the fuel source, leading to a decrease in the timber mass. Therefore, the adopted apparatus was required to be capable of analysing the combustion emissions while measuring the mass of the sample.

Additionally, an external heat flux was required to initiate the smouldering and this was required to be removed after a designated exposure time, to simulate fire extinguishment and allow for evaluation of self-sustained smouldering.

3.1 Materials

3.1.1 Timber Sample Materials

34mm thick pine was adopted for the timber samples. The density of the timber was calculated as 450kg/m^3 ± 20kg/m^3.

3.1.2 Encapsulation Materials

Two encapsulation materials were selected for the experiments. Firstly, plasterboard was selected due to its widely adopted use within industry for fire protection. Secondly, mineral wool insulation, due to its exceptional thermal insulation properties and positive results from Li (Li, 2022).

3.1.2.1 Plasterboard

12.5mm thick type A gypsum plasterboard in accordance with EN520:2004 (BSI, 2004) was chosen. The specific product was GTEC Standard board manufactured by Siniat. The plasterboard has a thermal conductivity of 0.19W/mK and an average density of 640kg/m^2 (ETEX, 2019).

3.1.2.2 Mineral wool

Mineral wool slabs of thickness of 50mm were utilised. The specific product was Rockwool Sound Insulation Slab. The insulation is stated as having a thermal conductivity of 0.038W/mK and a density of 45kg/m^3 (Rockwool, 2018). These were cut to the required thickness for the tested sample.

3.1.3 Insulation Materials

Mineral wool, the same as specified within section 3.1.2.2 was adopted for the sample's insulation.

3.2 Apparatus

3.2.1 Cone Calorimeter

The samples were tested using a cone calorimeter, in accordance with BS ISO 5660-1 (BSI, 2020) .

Figure 3: Cone Calorimeter utilised for testing

This apparatus collects the combustion gases from the ignited sample via its hood and extraction system. Samples are then drawn from the extraction ducting for gas analysis within the equipment. The Cone Calorimeter is capable of measuring the O_2, CO_2 and CO concentrations within the gases, while recording the volumetric flow. This allows for establishment of the HRR, based on the quantity of O_2 consumed (Babrauskas, 1984) or the concentration of CO_2. Full workings and description of the calculation process can be found within Babrauskas (Babrauskas, 1984). The samples are placed upon a load cell throughout the experiment, allowing for measurement of the sample mass, thus, determination of the mass loss rate. See Figure 3 for the utilised cone Calorimeter and Figure 4 for apparatus diagram.

The cone calorimeter has a controllable cone heater, capable of heat fluxes up to 100kW/m^2, which can be turned off when required. Therefore, the heater can be used to heat and ignite the samples for the desired exposure time and then turned off, simulating the fire extinguishment and allowing for evaluation if self-sustained smouldering is present. This can be orientated horizontally or vertically, allowing different axes to be evaluated.

Testing in accordance with BS ISO 5660-1 (BSI, 2020) states that the face of the sample shall be placed 25mm from the face of the cone heater. This creates a uniform heat flux over a 100mm [W] x 100mm [H] sample. Hence, the chosen samples were a maximum 100mm [W] x 100mm [H] to ensure the surface was evenly heated.

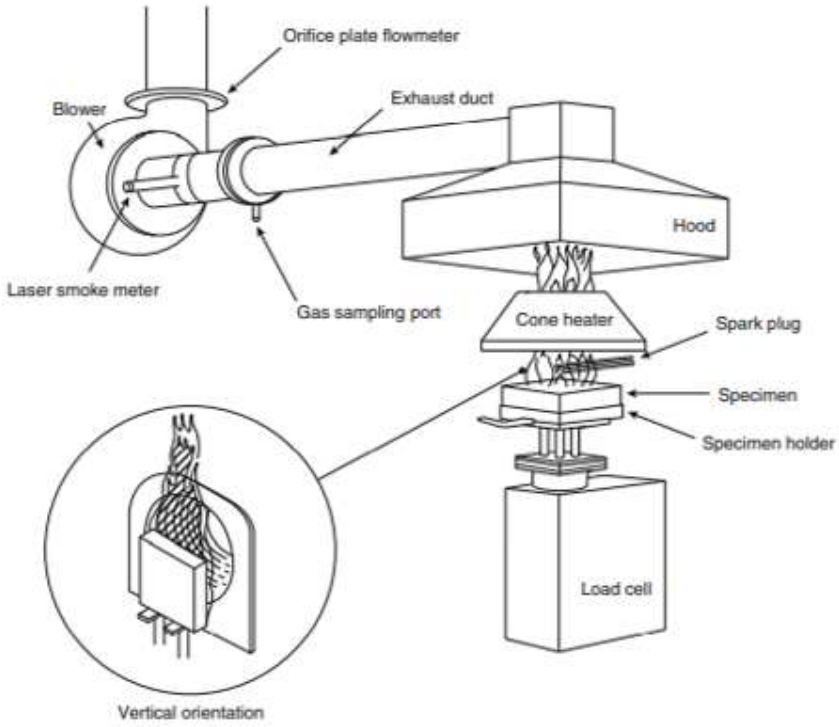

Figure 4: Cone Calorimeter apparatus diagram (Janssens)

3.2.2 Specimen Holder

The standard specimen holder in compliance with BS ISO 5660-1 (BSI, 2020) was unsuitable for our experiments, as the sides and back needed wrapped with insulation and the encapsulation material to the front. Therefore, a bespoke sample holder was constructed to accommodate the specimens, see Figure 5 for finalised sample holder.

Figure 5: Finalised sample holder used for the experiments

Due to proposed testing in the vertical orientation, the main design objective was to guarantee stability of the sample, ensuring it wouldn't fall over during or post heat exposure due to the degradation of materials, resulting in the end of the experiment. Additionally, the sample holder was designed to have minimal impact on the specimen, in regards to oxygen supply to the timber and heat losses from it.

The sample holder was constructed from Vermiculite boarding, a non-combustible material, due to its minimal reaction when heated. Furthermore, it was wrapped in shiny aluminium foil to protect it from the thermal radiation, via deflection, from the radiant heater.

To provide stability a clamping method was used, as seen in Figure 5. This compromised two vertical upstands, creating pressure on the sample's layers holding them together and providing stability. The upstands were attached to a horizontal member, via metal screws. The horizontal member was sufficiently sized to provide stability when situated on the load cell and create minimal torsion.

The adoption of the upstands omitted the need for positive fixings between the sample holder and sample. This was to omit the screws' acting as heat sinks and facilitating heat losses from the sample.

The front upstand was 22mm thick and flush with the front edge of the horizontal member. This allowed for the 25mm separation distance from the heater to the sample surface without any contact between. The rear upstand distance was dependent on the sample being tested, due to the varying thicknesses. Therefore, the back upstand was re-positioned per sample and screwed into the horizontal member where required.

The upstand's height was 35mm. This was to accommodate 30mm thick insulation to the bottom edge of the sample and 5mm up the front of the timber sample to provide the stability. Allowing for the 30mm insulation to the bottom was important to help reduce heat losses, while also allowing oxygen transport to the bottom to facilitate smouldering if present. The 5mm encroachment on the timber's front face would potentially block the radiant heat from the cone heater, however, this would be constant for all experiments and therefore deemed acceptable.

3.3 Procedure

The testing procedure was carried out as per below:

1. The cone calorimeter gas analyser was calibrated following University of Edinburgh calibration guide, which is in line with the requiems of BS ISO 5660-1 (BSI, 2020), but specific for the Edinburgh University machinery. This essentially involved zeroing and spanning the gas analysers for known flows of N_2 and CO/CO_2.

2. The samples were placed in the holder out with the cone calorimeter apparatus, with attention paid to confirm the samples were vertical and not angled. This was to ensure a uniform heat flux across the surface when exposed to the heater.
3. The sample holder was then placed onto the load cell and the height of the cone heater adjusted to provide uniform coverage. The sample holder was positioned to give 25mm from

the face of the heater to the sample and was aligned centrally. Once centred, the base was marked to allow for easy repositioning in the future and removed.

4. Calibration of the radiant cone heater to the desired heat flux. A water-cooled heat flux gauge was positioned centrally 25mm from the surface of the cone heater. The cone heater was set to the calculated temperature (°C) corresponding to the desired heat flux. Due to slight variations in the laboratory environment, the calculated temperature was not always the set temperature of the heater. Therefore, minor adjustments were made to the heater temperature to give the required heat flux within ±0.2kW/m^2. Once the cone heater was calibrated, the heat flux gauge was removed.

5. Once calibrated, the gas analysers were activated and air samples were drawn from the cone calorimeter. Also, the load cell started to record data. This was continuously done until the end of the experiment. The apparatus was left to record data for 60 seconds before the sample was placed within the cone calorimeter, in line with BS ISO 5660-1 (BSI, 2020) .

6. The holder was then placed upon the load cell, following the markings made within step 3, and exposed to the heat flux.

7. The samples were left exposed to the heat flux for the desired exposure time. This exposure time was prescribed one of two ways. The first, before the experiment, from literature and previous experiments. The second, due to the exploratory nature of the work, from analysing the live CO production and mass loss during the experiment to establish the time at which the wood sample was combusting. See section 3.4 for the criteria for smouldering.

8. At the end of the exposure time, the cone heater was set to 0°C. The cone heater requires time to cool down to ambient levels. For the cone heater used, it takes approximately 10 minutes for the heat flux to reduce from 50kW/m^2 to 6kW/m^2 (Li, 2022). 6kW/m^2 has been found to be the minimum heat flux for self-extinguishment of solid timber (Crielaard et al., 2019).

9. The experiment was ended once the smouldering had ceased. The criteria for this were when the CO concentration become 0PPM and there was no mass loss from the sample.

3.4 Criteria For Smouldering

There are three main indicators that timber is smouldering. Firstly, a rapid increase in temperature exceeding 300°C is observed, correlating to the exothermic oxidation reaction taking place (Fangrat et al., 1996). Secondly, a significant and sharp increase in CO yield (Ronda et al., 2016). Thirdly, a positive

mass loss rate, highlighting the fuel source being consumed. These criteria shall be used to evaluate when the samples start smouldering and how long it continues for.

The smouldering shall be considered extinguished once the CO falls to an ambient level and there is no more mass loss.

3.5 Samples

All timber samples were 90mm [W] x 90mm [H] x 34mm [D], within the maximum dimensions of 100mm square to ensure an evenly distributed heat flux.

As seen from previous experimental work (Su et al., 2018a) (Wiesner et al., 2021) (Kotsovinos et al., 2023), the presence of joints was commonly observed when sustained smouldering was present. These joints created an energy feedback system between the smouldering timber faces, helping to sustain the combustion.

To replicate similar conditions and joints between CLT panels, the timber samples had a 1mm wide vertical cut through the entire depth of the sample. This vertical cut was centred on the timber, hence, 45mm from the sides. The timber was not cut for the entire height of the sample, which would result in two smaller sections. Instead, a 10mm high section remained uncut at the bottom of the sample. This was to ensure that the gap would remain constant during the experiment. From preliminary trials, when the timber was fully cut creating two smaller sections, during the sample assembly the pieces could move freely, either closing the 1mm gap or remaining in place. Therefore, for continuity, it was opted to leave the small section uncut, resulting in all samples with a standardised gap of 1mm.

Figure 6: Sample showing the vertical cut

As discussed, minimising heat loss from the timber is critical for smouldering, thus, each sample had insulation wrapping to its edges and rear face. As the main objective of the testing was to research into the effect of encapsulation, all samples implemented the same specification for the side and rear

insulation. A prevailing variable in the experiments by Li (Li, 2022), was that sustained smouldering was observed with the adoption of 25mm thick mineral wool insulation to the sides and rear. When insulated with aluminium foil, no sustained smouldering was present. Hence, our samples were all wrapped in 30mm thick mineral wool insulation, as specified in section 3.1.3. This material would allow oxygen transport to the reaction zone, while reducing the heat losses. As the chosen thickness surpasses that of Li (Li, 2022) it gave confidence that the adopted arrangement would be sufficient to create positive conditions for sustained smouldering.

To form the insulation, 150mm x 150mm sections were cut from 50mm thick mineral wool insulation slabs and a 90mm [W] x 90mm [H] x 34mm [D] central void was cut out. This created a pocket in which to place the timber sample, ensuring a tight fit with no gaps between the timber and the insulation, giving the desired 30mm side insulation. The faces of the timber and insulation were flush.

Figure 7: Insulation pocket adopted for all samples

To create the 30mm rear insulation, a separate 150mm [W] x 150mm [H] x 50mm [D] section was trimmed down to 16mm thick and was layered behind. This gave the required 30mm thick rear insulation. To hold the two pieces together, a 1mm diameter steel wire was threaded through the top

Figure 8: Method utilised for joining the additional rear insulation

corners and hooked together, see Figure 8. This, along with the clamping method from the sample holder, held the two pieces firmly in place, not allowing any separation.

The encapsulation materials were cut to 150mm [W] x 150mm [H] sections, providing coverage to the timber and the insulation wrapping, instead of adopting 90mm x 90mm to only cover the timber section. This helped protect the insulation from thermal degradation during the exposure time and provided stability to the sample.

From initial trials, when an encapsulation section of only 90mm [W] x 90mm [H] was implemented, the timber sample became unstable and on numerous occasions was observed to fall out of the pocket created within the insulation. This resulted in major heat losses and posed a problem for uniformity across experiments. Therefore, to avoid this issue, a section of 150mm [W] x 150mm [H] was trialled and implemented. This was seen to provide stability, as the encapsulation material was sufficiently clamped and held in place due to the sample holder uprights.

(a)

(b)

Figure 9: (a) Trial sample configuration with 90mm x 90mm encapsulation, leading to instability. (b) Final sample, adopting encapsulation size of 150mm x 150mm

3.6 Test Matrix

The experimental test matrix is shown in Table 2.

3.6.1 Experiments 1-6

Experiments 1-6 were to investigate the difference in behaviour due to varying encapsulation materials. Hence, each sample had a different material or thickness for encapsulation. The chosen materials were mineral wool and plasterboard with 1 to 3 layers tested. All materials were in accordance with the specification in section 3.1. All samples were exposed to the same heat flux of 50kW/m^2.

As the testing was to investigate conditions for sustained smouldering post heat exposure, it was necessary to cause the timber sample to ignite. This resulted in differing exposure times for each

experiment. During the exposure time, the CO yield and mass was continuously monitored. Once we were confident the timber had ignited and was smouldering, the cone heater was turned off. This was based on the criteria stated within 3.4 and allowing a nominal period of time after assumed ignition to guarantee the sample was smouldering.

Experiment 2 adopted the same method for holding the encapsulation material in place with the additional layer of insulation to the rear. This resulted in constant contact between the timber and encapsulating material with no airgaps.

Experiments 3a – 5b utilised 2 no. Ø3.35mm x 35mm screws to fix the plasterboard in place. The screws were centrally located either side of the vertical cut. Only two fixings were selected for numerous reasons. Firstly, due to the small scale of the sample, edge distances and spacings for the fixings could not adequately be adhered to for a greater number of fixings (BSI, 1995). This could lead to the possibility of creating fissures in the timber, which would go unnoticed, being hidden behind the plasterboard, and could impact the results. To help mitigate this risk for two fixings, all holes were pre-drilled. Secondly, the metal screws have a high thermal conductivity and, thus, would act as a thermal sink, easily absorbing energy from the timber sample, resulting in greater heat losses. As a result, a minimal number of screws was desirable. Thirdly, two screws were sufficient in providing stability to the material throughout the experiments, keeping the plasterboard fully fixed and in contact with the timber sample.

Experiment 6 adopted the same number and spacing of screws as above. But, due to the thickness of 3 layers of plasterboard, the previous screws were too short to penetrate into the timber. Consequently, they were swapped for Ø3.35mm x 50mm screws, which provided adequate penetration into the timber sample.

3.6.2 Experiments 7-10

This range of experiments was to investigate the effect the imposed heat flux could have on the sustained smouldering. For that reason, experiments 7-10 all utilised a single layer of plasterboard, with the fixing method the same as experiments 3a-5b. Again, the exposure time varied per experiment to ensure that the timber was smouldering. From the onset of smouldering, based on the criteria in section 3.4, the cone heater was set to zero after 15 minutes.

3.6.3 Individual Encapsulation Materials

Each of the encapsulating materials were independently tested within the cone calorimeter in order to evaluate their reaction when exposed to a heat flux. This was done for a heat flux of 50kW/m^2, with the exposure times matching that of the experiments corresponding to that material.

Table 2: Test matrix

Experiment Ref	Timber Sample	Encapsulation Material	Heat Flux (kW/m^2)	Exposure Time (Min)
1	90x90x34mm Pine	None	50	15
2	90x90x34mm Pine	Mineral wool	50	20
3a	90x90x34mm Pine	1 layer of plasterboard	50	20
3b	90x90x34mm Pine	1 layer of plasterboard	50	20
4a	90x90x34mm Pine	1 layer of plasterboard	50	30
4b	90x90x34mm Pine	1 layer of plasterboard	50	30
5a	90x90x34mm Pine	2 layers of plasterboard	50	75
5b	90x90x34mm Pine	2 layers of plasterboard	50	75
6	90x90x34mm Pine	3 layers of plasterboard	50	150
7	90x90x34mm Pine	1 layer of plasterboard	40	35
8	90x90x34mm Pine	1 layer of plasterboard	30	38
9	90x90x34mm Pine	1 layer of plasterboard	20	52
10	90x90x34mm Pine	1 layer of plasterboard	75	30
MW	-	Mineral wool	50	20
1PB	-	1 layer of plasterboard	50	30
2PB	-	2 layers of plasterboard	50	75
3PB	-	3 layers of plasterboard	50	150

4 Results Analysis and Discussion

The experiment results and data analysis shall be presented within the following chapter. The experiments have been split into three data sets, depending on the main variable being investigated. The results from the individual encapsulating materials exposed shall be presented as data set 1. This is to provide insight into the effect the thermal decomposition of the encapsulating materials will have on the results. Data set 2, shall present the results where the main variable investigated was the exposure heat flux. While data set 3, shall focus on the encapsulation material.

First, general observations and issues occurred shall be presented for all, followed by results from the specific data sets.

4.1 Experiment Observations

All experiments were completed without any significant issues. The samples remained stable, with a select few experiencing very minor rotations forward during the experiment, resulting in a not fully vertical face. This was only observed after the heat flux was removed, meaning the samples were still evenly heated during their exposure. From what could be observed, the encapsulation materials remained in full contact with the insulation wrapping, hence, the timber was assumed to remain fully insulated during the experiment.

Due to the experimental run time, drift was observed in the CO analyser for experiment 4a, 7, 8 and 9. This was confirmed via terminating the experiment and data logging, removing the sample from the apparatus and running an empty experiment without calibrating the apparatus. The measured CO concentration remained at the same levels as the end of the experiments. The drift observed was minor, with a maximum value of CO 1.9PPM. When determining the smouldering extinguishment, this was accounted for.

All but two experiments were able to run until the smouldering extinguished. Due to laboratory limitations, experiments 6 and 9 had to be terminated after 6 hours 24 minutes and 7 hours 1 minute respectively. Both samples were still smouldering at the time of termination. The samples were removed from the testing apparatus and the encapsulation material carefully removed to expose the timber underneath. Figure 10(a) and (b) shows the remaining charred timber for experiment 6 directly after termination, with various points observed to be glowing orange, confirming smouldering. Afterwards the timber was placed back in the insulation wrapping with the encapsulation material still attached. The samples were positioned vertically in the sample holder and left for 18 hours. The encapsulation was again removed, to expose the timber. As seen in Figure 10(c) and (d), the remaining

char was still located around the screws, however, the resultant mass was substantially less. This indicates the that char continued to oxidise after the experiment termination.

(a) *(b)* *(c)* *(d)*

Figure 10: (a), (b) – Remains of experiment 6 immediately after termination of experiment; (c), (d) – Remains of experiment 6, 18 hours after experiment termination after being left in with encapsulation and insulation wrapping

Experiment 5b experienced problems regarding the stability of the plasterboard and timber. As shown in Figure 11, the plasterboard rotated forward by a substantial amount about the base of the sample, leading to separation from the insulation wrapping. As the timber was fixed to the plasterboard, this in turn displaced it from the pocket formed in the insulation leaving sections of its side exposed. The timber could visibly be seen smouldering, with the char glowing orange. As the experiment was running the separation distance could not be accurately measured, but appeared to be in the region of 1-3mm, with the greatest separation observed along the top edge, due to being furthest away from the point of rotation.

As the timber edges were slightly exposed, this would have resulted in greater heat losses to the environment, impacting the smouldering characteristics. The heat losses due to this issue cannot be quantified due to the experimental set-up, but needs to be considered when reviewing the results.

Figure 11: Experiment 5b falling forward, leading to minor section of exposed timber

Experiment 6 experienced problems with the plasterboard stability, however this was a different issue from that observed in experiment 5b. As expected, when the plasterboard underwent thermal exposure, it started to thermally decompose, as explained within section 2.2.3. However, due to the long exposure time in experiment 6, the plasterboard started to lose its structural integrity, specifically the outer layer, as this was heated the greatest. The plasterboard developed horizontal cracks at various points across its height. This resulted in the outermost layer falling forward, losing contact with the second layer, as shown in Figure 12(a) and (b). This gap was measured as 0.5-3mm and only present for the top half of the layer, above the fixings. Below the screws, there was no gap and the plasterboard layers remained in contact.

(a) *(b)*

Figure 12: Plasterboard thermal degradation seen in experiment 6 leading to partial separation between the outer most and middle plasterboard layers: (a) During heat flux exposure: (b) Post heat flux exposure

Thermal degradation of the plasterboard was observed for all experiments utilising plasterboard. The paper layers were consumed during the experiment, leaving ash behind. Significant horizontal and vertical cracking was observed for all layers of plasterboard. The widest cracking was measured as 2mm, with the majority being 0.5-1mm. Cracks were seen to pass through the location of the screws, which appeared to be the originating points for the majority.

No sustained flaming was observed for any experiments with encapsulation. The only flames witnessed was in experiment 1, when the timber was exposed. Once the heat flux was removed, the flames extinguished and no re-ignition was observed.

Towards the end of the experiments, typically within the last 10 minutes, a minor increase was seen in the mass of the samples. It is believed that this was caused by moisture gain in the samples from the atmosphere, which has been observed in other experimental research projects.

Figure 13: Thermal degradation of plasterboard observed for experiments

4.2 Data Issues

4.2.1 CO_2 and O_2 Analyser

The O_2 concentration was expected to reduce below ambient levels as the samples smouldered, as a result of the oxidation reaction depleting the O_2 levels in the combustion gases. However, as seen on Figure 14(b) and Figure 15(b), in the majority of the experiments the O_2 concentrations steadily increased during the experiments, exceeding ambient levels. This would have required an external source of O_2, which was not provided. As this was not an isolated incident, the O_2 analyser was considered faulty.

A similar issue was observed for the CO_2 analyser. As discussed in section 2.1, smouldering combustion would produce CO_2, albeit, at a lower ratio than flaming combustion. However, numerous experiments measured CO_2 levels lower than the ambient air as the experiments continued. Additionally, experiments 4, 6 and 10 all dropped to 0PPM during the experiment, when visible combustion gases could be seen emitting from the sample, see Figure 14(a) and Figure 15(a). The current atmospheric levels are 300-400PPM (Change, 2023) dependent on the surrounding environment, which highlights a fault with the CO_2 analyser.

Due to this, the reliability and accuracy of the measured concentrations for O_2 and CO_2 cannot be guaranteed and are considered unsuitable. Hence, no further discussion or analysis shall be made, meaning no calculation of the HRR could be completed.

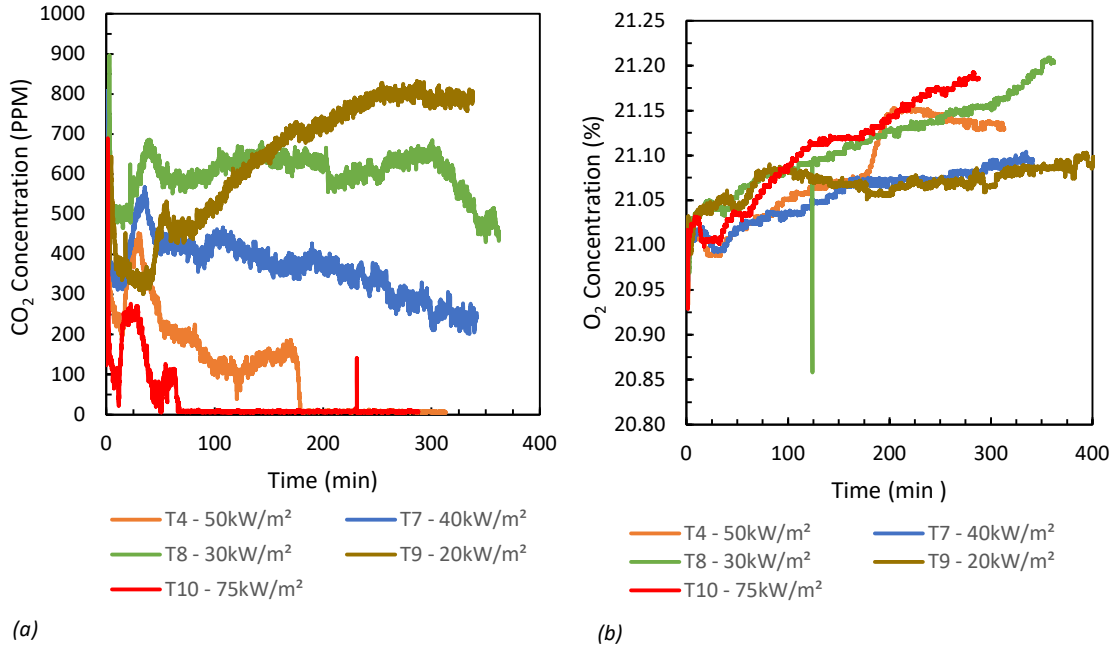

Figure 14: Data set 2 – (a) Measured CO2 concentration; (b) Measured O2 concentration

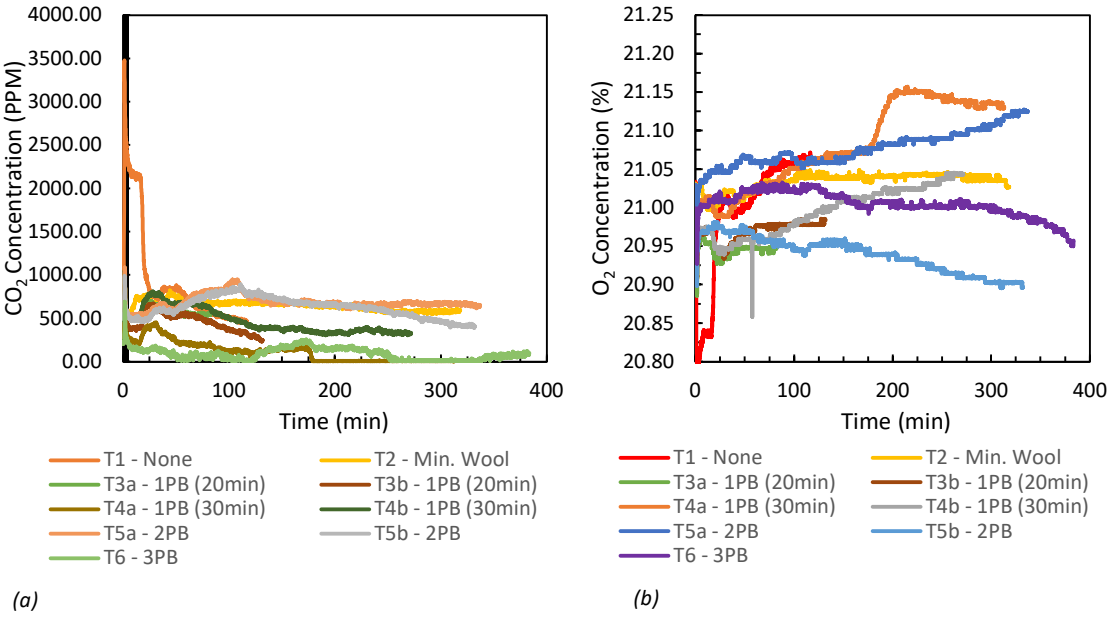

Figure 15: Data set 3 – (a) Measured CO2 concentration; (b) Measured O2 concentration

4.2.2 Data Logging

Due to unforeseen circumstances, the data logger was shut down during experiment 3b. Therefore, only 132 minutes of data has been recorded and is analysed. From review of the data it was apparent the sample was smouldering at the time of experiment termination.

Due to user error, the sample weight was not recorded for experiment 4b. The CO concentration was still measured, hence, analysis of the production rate, ignition and smouldering time was still completed.

From analysis of the mass for experiment 5b, the values had many minor fluctuations, but still showed an overall reducing mass. The effect of these fluctuations can be seen on Figure 35. The observed results shows evidence of vibration affecting the sample, consequently it is believed that the sample holder may have had slight contact with the cone heater. As a result, when analysising the values for the MLR and CO yield, caution was applied to ensure the fluctuation values were not interpreted. The CO production rate, ignition time and smouldering time are unaffected by this.

4.3 Data Set 1 – Individual Encapsulation Materials

Figure 17 and Figure 16 presents the CO production rate and MLR for the individual encapsulating materials. The experiments were run for the maximum exposure time from the experimental matrix, corresponding to that material when subjected to a 50kW/m^2 heat flux. For the mineral wool this was 15 minutes, 1 layer of plasterboard 30 minutes, 2 layers of plasterboard 75 minutes and 3 layers of plasterboard 150 minutes. The testing was stopped at these times, as past this when the heat flux was set to zero there would be minimal reaction of the encapsulating materials, as the only external source would be the smouldering timber, which couldn't be quantified. This was deemed to have negligible effect to the encapsulating materials, which would have been exposed to greater heat flux for a significant time period, resulting in the majority of its thermal degradation.

The main interest was establishing the effect the encapsulating material had on the CO concentration and mass loss, to allow accurate determination of ignition times.

The mineral wool was least impacted, with a peak CO production rate of 0.00015g/s and MLR of 0.31g/m^2s at 1.5 minutes, with a return to ambient levels by 3 minutes, where it remained for the remainder of the experiment.

The plasterboard layers showed close alignment for the growth, decay and stabilised regions for all experiments when looking at the CO production and MLR. An initial peak in the CO production is seen,

0.00072 - 0.00084g/s. This was observed within the first 6 minutes. After this, the single layer levelled off at 0.000020g/s and remained constant until the end of the experiment. The double and triple layer stabilised at this level as well, until 22 minutes, when both production rates increased, forming a small plateau before decaying. The double layer returned to 0.000020g/s by 49 minutes and remained constant there until the end of the experiment. The triple layer stabilised at a slightly greater rate of 0.000025g/s, where it remained until 70 minutes. Its production rate started to gradually increase up to a high of 0.000050g/s and then reduced to 0.000022g/s at 107 minutes, where it remained constant until the end of the experiment. Due to their alignment, the first peak is attributed to be the reaction of the first plasterboard layer, while the small plateau is the second layer and the final small increase and decay is the third layer.

The final stabilised CO production and MLR are insignificant for the plasterboard and mineral wool, with a maximum of 0.000025g/s and 0.031g/m^{2}s respectively. Consequently, it is deemed to have negligible effect on the results for the following data sets.

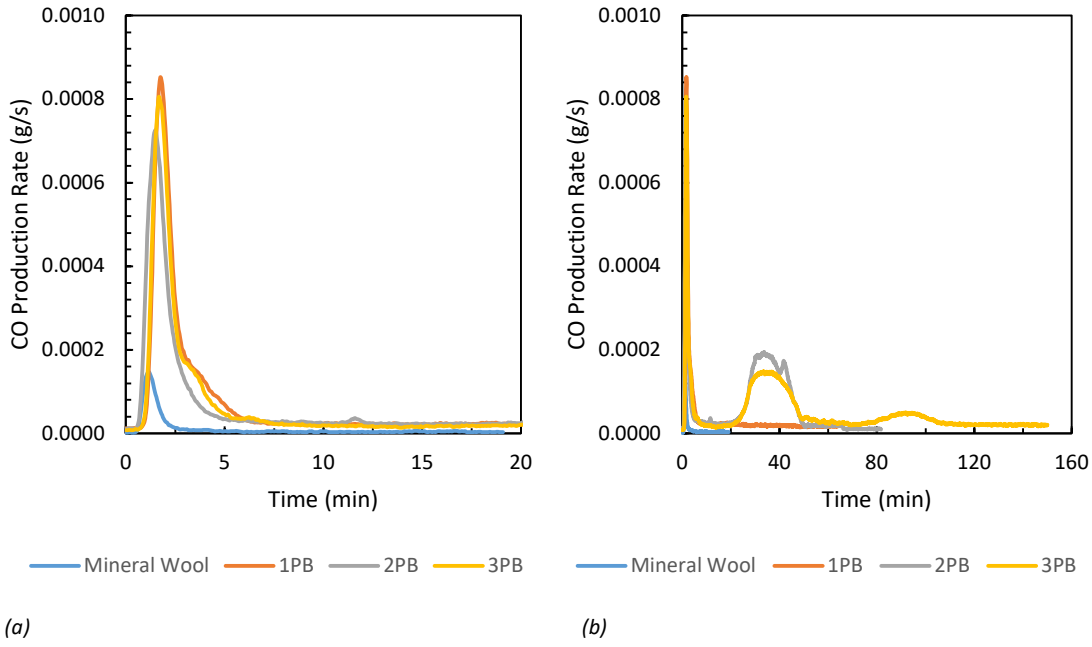

Figure 16: Data set 1 - CO production rate against time. (a) Reduced time frame to highlight initial reaction: (b) Full exposure time

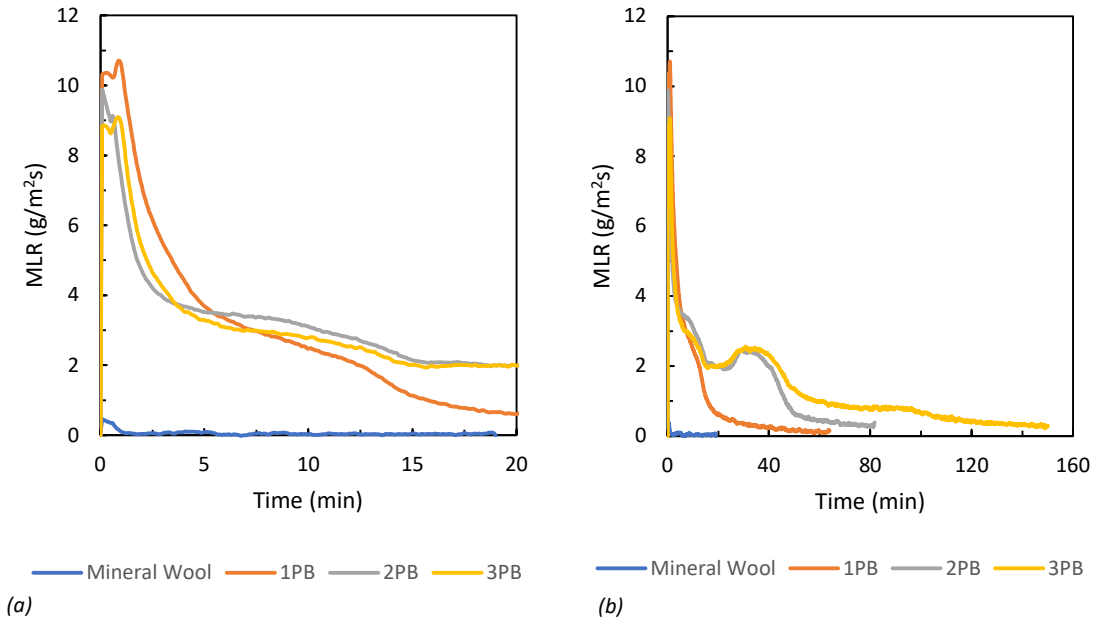

Figure 17: Data set 1 - MLR against time. (a) Reduced time frame to highlight initial reaction; (b) Full exposure time

4.4 Data Set 2 – Varying Exposure Heat Flux

Table 3 states the experiments to be presented within data set 2 and their corresponding variables. All experiments utilised a single layer of plasterboard, but with a varied heat flux.

Table 3: Experimental variables for test within data set 2

Experiment Ref	Encapsulating Material	Exposure Time (min)	Heat Flux (kW/m^2)
10	1 layer of plasterboard	30	75
4	1 layer of plasterboard	30	50
7	1 layer of plasterboard	35	40
8	1 layer of plasterboard	38	30
9	1 layer of plasterboard	52	20

4.4.1 Ignition Time

Figure 18 presents the CO concentration and Figure 19 presents the MLR during exposure time. This is the time in which the experiment is ignited. For clarity, the figures have been repeated only showing the first 10 minutes to highlight the reaction of the single layer plasterboard.

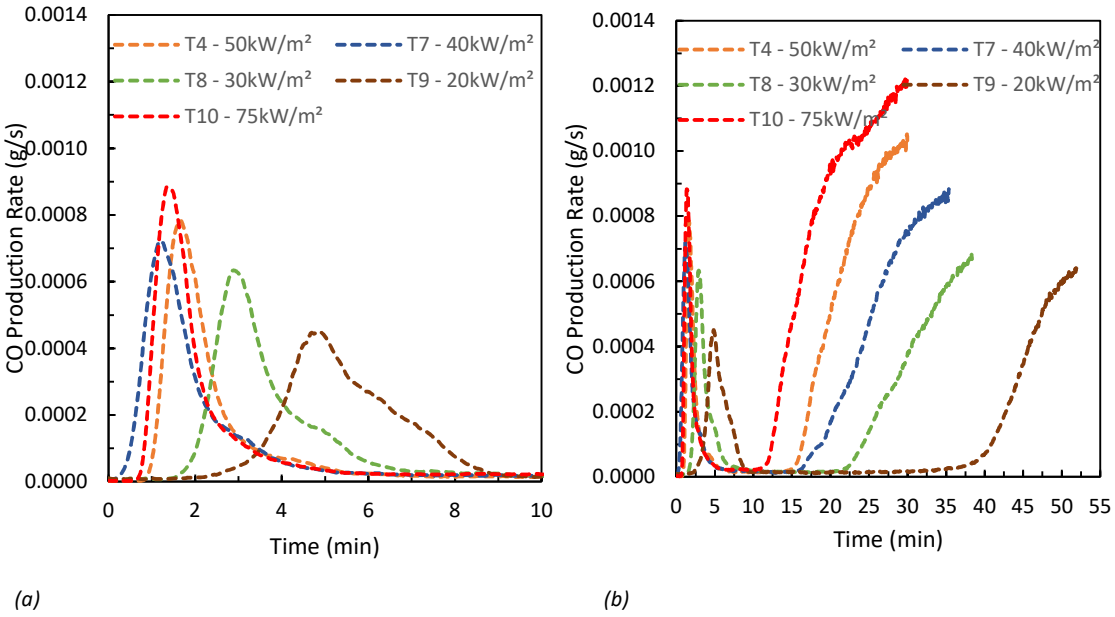

Figure 18: Data set 2, CO production rate during heat flux exposure. (a) Reduced time frame to highlight initial reaction: (b) Full exposure time

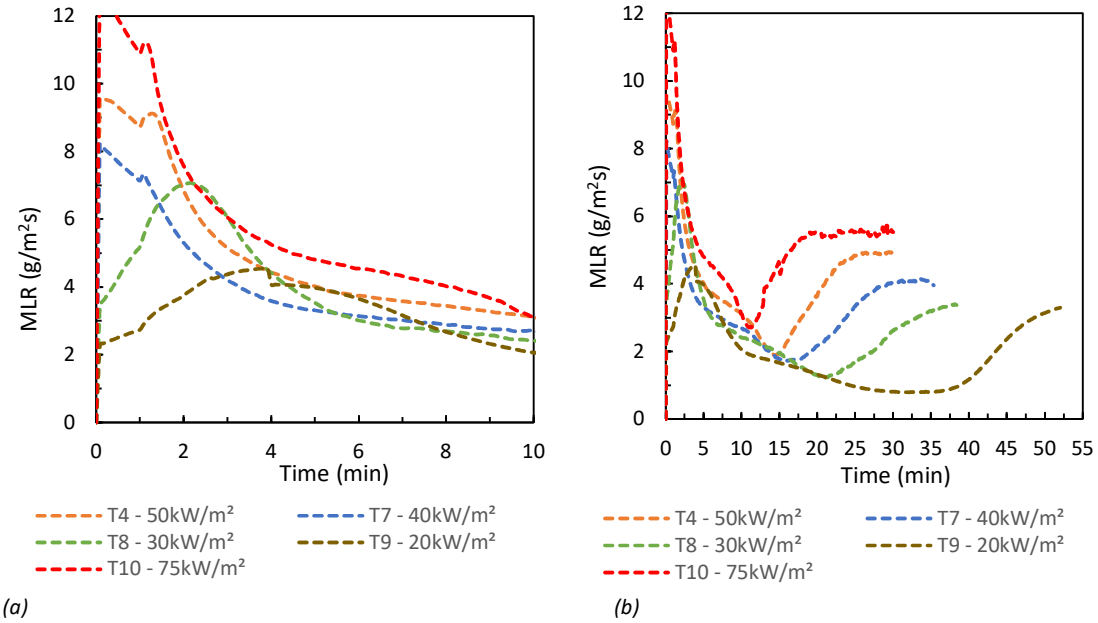

Figure 19: Data set 2 MLR during heat flux exposure. (a) Reduced time frame to highlight initial reaction: (b) Full exposure time

Data set 1 tested the effect of the individual encapsulating materials when exposed to a 50kW/m^2 heat flux. This allowed for a direct comparison for data set 3, however here, due to the varying heat fluxes, no specific testing has been complete. Nevertheless, from its testing and data set 3 results, we know the first peak in the CO rate, observed at 0-10 minutes for the experiments is due to the reaction of the plasterboard when first exposed to the heat flux. After the peak, the production rates rapidly decrease and all experiments are at the levels seen in the steady state region from data set 1. The maximum peak was 0.00088g/s when exposed to 75kW/m^2 and occurs the fastest at 1.4 minutes. As the heat fluxes reduce, the time for the plasterboard reaction increases. Additionally, the rate of change for CO concentration decreases, with a lower peak measured and the time before the concentrations return to ambient levels increasing. This can be seen from experiment 9, the lowest heat flux tested 20kW/m^2, which takes the longest time before the production rate increases. And when it does, it is at a significantly slower rate, with a drastically lower peak and observed over a longer period of time.

The initial reaction of the encapsulation material is also seen in the MLR. During the exposure time, there is a peak followed by a rapid in the MLR, before it swiftly increases again highlighted in Figure 19(b). The peak is attributed to the thermal degradation of the plasterboard, with the mass loss resulting from the burning of the facing paper, which happens over a very short period of time. The MLR then drops off, but doesn't reduce to 0g/m^{2}s. As the plasterboard temperature increases, the moisture within begins to evaporate, resulting in mass loss and subsequently establishing a positive MLR. This process takes time, hence the decay. After a while, an increase in the MLR is observed. This point can be linked to two factors. First, the burning of the paper layer to the rear face of the plasterboard and secondly, the pyrolysis and oxidation reaction of the timber sample. It is impossible to differentiate between these factors during the observed growth, but it is believed that the burning of the paper would precede the pyrolysis of the timber.

Post the initial effect of the encapsulating materials, the experiments all exhibited the same pattern. A negligible or zero CO production rate, with a rapid increase once ignition occurred, as seen on Figure 18. The rapid increase is a result of the oxidation reaction which has a high CO ratio (Rein, 2009). This is reinforced by the mass loss rate, which transitions to an upward trend 1-3 minutes prior to the increase in CO production rate. This delay can be attributed to three main factors. Firstly and most importantly, the timber will undergo pyrolysis before oxidation, due to the lower temperature required, breaking down the fuel resulting in pyrolysate gases being emitted and reducing the mass. The oxidation reaction will succeed this, resulting in the increased CO later. Secondly, the time delay for analysing the gases which is stated at 35 seconds for the specific apparatus used compared to the

load cell which is instantaneous. Finally, the time required for the combustion gases to travel from the burning sample, to the extraction ducting and the sampling point.

Changes in the trends are more obvious from the CO production rates. Due to this, the ignition times shall be based on it, with the mass loss rate used to confirm or provide supporting evidence if required. To allow for unity and equal comparison between the experiments, a minimum threshold has been selected for the identification of smouldering. Once the CO production rate increases above 0.0001g/s, after accounting for the encapsulation material's reaction, ignition is assumed. This criterion shall be adopted for data set 3 as well.

Table 4: Data set 2 - experimental ignition times

Experiment	Exposure Heat Flux (kW/m^2)	Ignition time (min)
10	75	12
4	50	16
7	40	19
8	30	24
9	20	40

The ignition times are listed in Table 4, As seen the 75kW/m^2 heat flux had the quickest ignition, with 20kW/m^2 the slowest. In between, the ignition times decreased with an increasing heat flux.

As expected, the higher heat fluxes posed the quickest ignition times. A greater quantity of energy was able to be transferred to the plasterboard within the same time period. This increased energy, quickened the dehydration process and thermal degradation of the plasterboard. Thus, as all experiments had 1 layer of plasterboard, resulted in faster heat transfer through the material, and subsequently to the face of the timber sample. Resulting in a quicker ignition time.

The ignition times for the corresponding heat fluxes are plotted on Figure 20. This highlights that there is a non-linear relationship between the heat flux and ignition time.

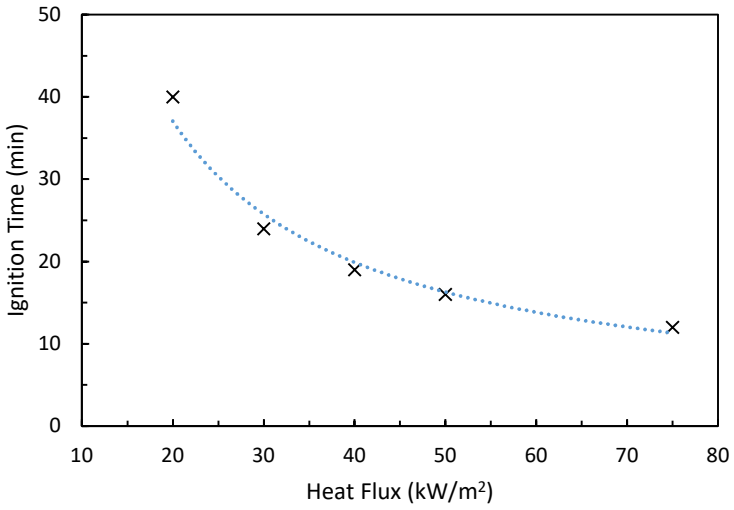

Figure 20: Ignition times for timber protected with a single layer of plasterboard against heat flux

4.4.2 Smouldering Characteristic

Figure 21 present the CO production rate, Figure 22 the MLR and Figure 23 the CO yield for the experiments within data set 2, all displaying a similar trend.

As discussed in section 4.4.1, the initial peak observed for the CO production rate within the first 5 minutes is attributed to the plasterboard's initial reaction to the heat flux. Once the heat flux is removed, the CO production rate increases for a nominal period of time, 1 – 3 minutes, after which a rapid decay is observed. This reverts and transitions back into an increasing production rate up to a second peak, where it starts to decay again. Afterwards, the CO production rate begins to stabilise, with a very gradual reduction rate observed for an extended period of time.

A similar pattern can be seen to occur for the MLR, with the growth and decay periods near aligning. For experiments 4, 7 and 10 a small plateau can be seen in the MLR during the exposure phase at 4.9g/m^{2}s, 4.1g/m^{2}s and 5.5g/m^{2}s respectively. Due to this, the timber can be assumed to be smouldering at a steady state, with aid from the cone heater.

Post heat flux removal, the MLRs for the experiments increase momentarily, but then decrease at an accelerated rate. Once the cone heater has been set to 0kW/m^2, it requires a period of time to cool down to below 6kW/m^2, the lowest external heat flux for timber's self-extinguishment (Crielaard et al., 2019). For the 50kW/m^2 experiment this time was measured as 10 minutes. Hence, within the first minutes post removal, the samples are still subjected to a significant heat flux, resulting in the continued increase in MLR but at a much slower rate. Once the cooling heat flux to the samples

reduces below a certain level, the increasing MLR can no longer sustain itself and the decay is witnessed. This can be seen within the experiments, with the higher heat fluxes continuing to increase slightly longer post removal than samples exposed to the lower fluxes.

As the heat flux reduces and falls to 0kW/m^2, the energy required for the pyrolysis of the timber comes only from the exothermic oxidation reaction, which produces significantly less energy than the original external heat flux. So naturally, the MLR decreases.

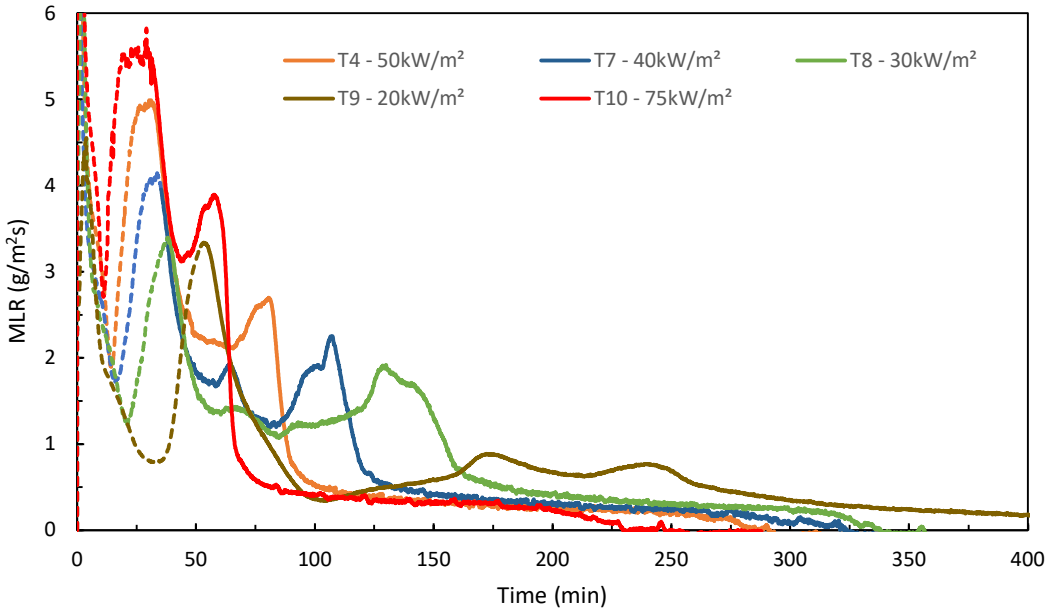

Figure 21: Data set 2 experiments - CO production rate

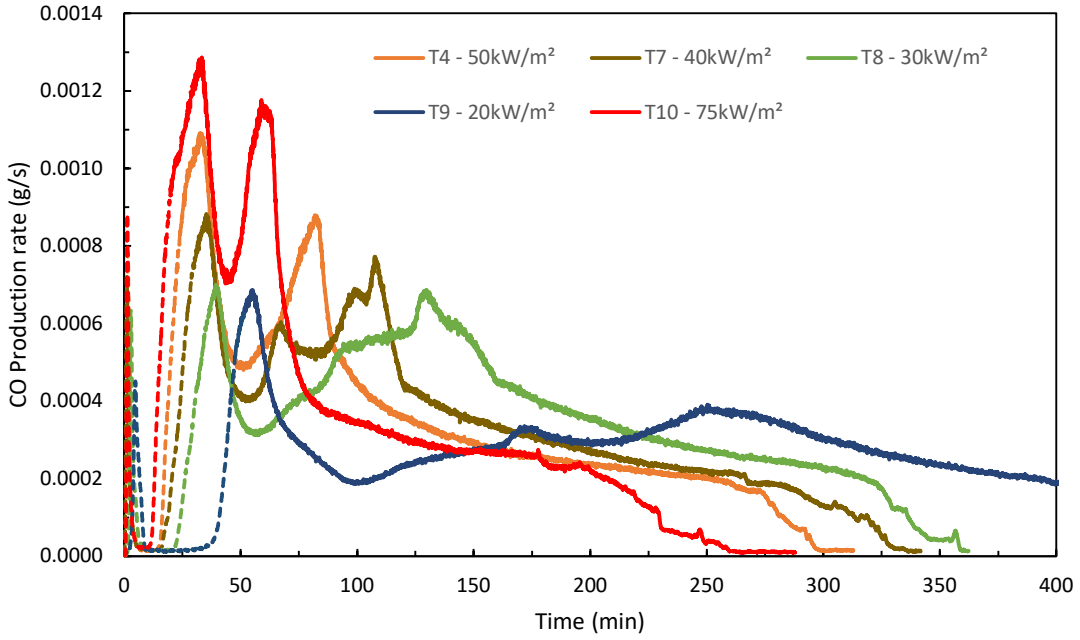

Figure 22: Data set 2 experiments - MLR

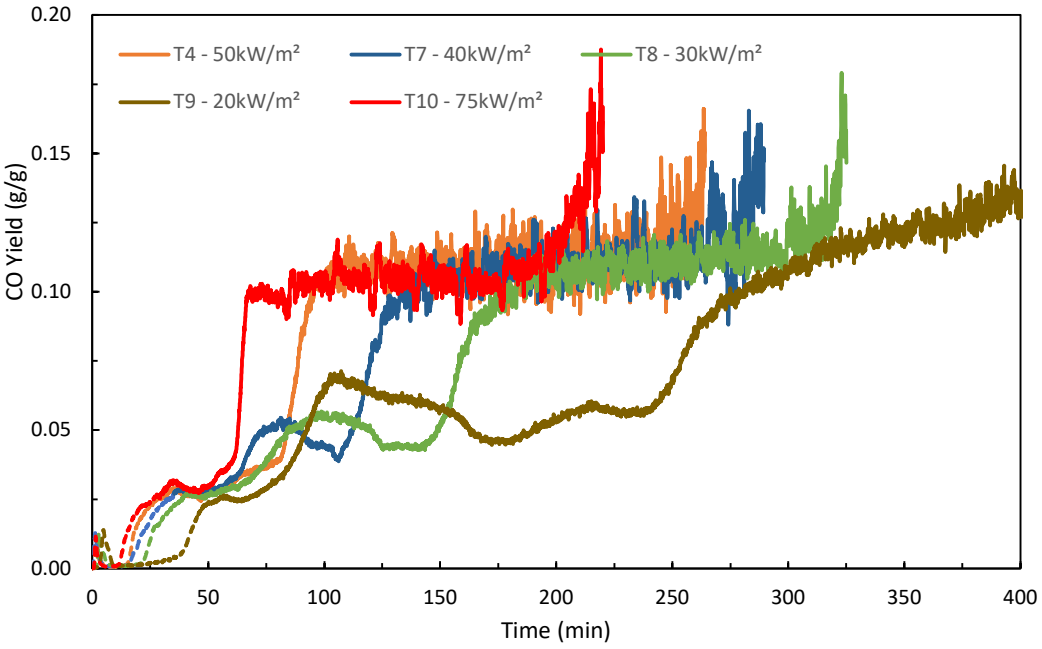

Figure 23: Data set 2 experiments - CO yield

From the initial decay post the heat flux removal, the MLR shows signs of stabilising, with varying periods of a semi-constant MLR depending on the exposure heat flux. This constant MLR highlights that the timber is smouldering at a semi-steady state. This differs from the CO production rate, which shows no sign of remaining constant, instead reverting to a growth pattern almost instantaneously.

After which, the MLR transitions to a growth phase, creating a second peak, matching the observed trend for the CO production. However, the second peak for the MLR is always considerably lower, not aligning with that of the CO production. After this final peak, the MLRs all rapidly decay and then stabilise, where they remain constant for an extended period of time, until a final gradual decay to 0g/m^{2}s is seen.

For each aspect of the data represented, there are clearly two distinctive regions which correlate with the decay and growth of one another. Taking experiment 8 for example, the first plateau, averaged at 1.30g/m^{2}s, is believed to be the result of steady state smouldering of the timber, with both the pyrolysis and oxidation processes occurring simultaneously. This plateau is well beyond the time the reducing heat flux would have influence and is also seen on the CO yield figures.

As these fronts move deeper into the timber, so does the heat transfer ahead of them. However, there comes a point in time, where the heat transfer ahead of the pyrolysis front reaches the rear of the timber sample. Due to the tight fitting back and side insulation, the heat cannot be easily lost to the environment and due to its low thermal conductivity, will not be transferred away at the same rate

heat is produced from the oxidation reaction and transferred to it. Thus, creating conditions where the internal energy of a finite mass of timbers will rapidly increase. This can be deemed as the transition from thermally thick to thermally thin.

With this continuously increasing energy and minimal heat losses in the finite timber section, the temperature increases at a greater rate, leading to an increased rate of pyrolysis and subsequently MLR. This can be correlated to the second rapid growth seen in the MLR graphs, which for experiment 8 is at 120 minutes. This issue is compounded by the propagating pyrolysis front, reducing the area of unburnt timber, resulting in an even greater energy imbalance.

As pyrolysis occurs at lower temperatures than the oxidation, the remaining sections of unreacted timber underwent pyrolysis first, resulting in char formation and pyrolysate gases being emitted. It has been found that that the pyrolysis of timber accounts for the largest percentage of observed MLR for timber samples, while the char oxidation accounted for the least (Richter et al., 2021) (Morrisset et al., 2021) (MacLeod et al., 2023). Hence, once the timber has been fully pyrolysed, the MLR is expected to reduce.

Based on this, the location of the second peak, 125 minutes for experiment 8, can be seen as the point when the vast majority of the timber has been pyrolysed and the rapid decay is witnessed due to the char oxidation becoming the dominating reaction.

The gradient of the decay can be used as a guide to the volume of unreacted timer. When a steeper decline is observed, such as experiment 4 and 10, there is less unreacted timber, hence a greater rate of change due to the MLR from char oxidation being considerably less. Compared to experiments 7 and 8, where the decay is shallower, due to a greater mass of uncharred timber being pyrolysed, resulting in a smaller rate of change. Albeit, this is qualitative description and the percentage of charred to uncharred timber cannot be established.

The final stabilised region for the MLR, seen in experiment 8 from 180 minutes onwards, can therefore be classified as predominantly a char oxidation phase. However, the pyrolysis and oxidation reactions cannot be fully uncoupled based on the analysis, consequently, there could still be sections of uncharred timber. Based on the vastly different resultant MLRs, however, we are fairly confident that this is predominantly char oxidation.

This is reinforced by the lack of major fluctuations, with a fairly constant value seen for an extended period of time. The oxidation rate of the char is dependent on the supply of the oxygen to the reaction zone and, since it is an exothermic reaction, is not influenced by the energy supplied. The samples adopted the same insulation wrapping with plasterboard to the front, hence, the oxygen supply to the

char will be nigh on identical. This is reflected across all the experiments within this data set, with their MLR all in the range of 0.3g/m^{2}s ±0.003g/m^{2}s.

The growth and decay transitions, along with the semi-steady states from the MLR, are reflected on the CO yield figures. Moreover, the CO yields show a more obvious and longer stabilised region, relating to the semi-steady state phases described above. The CO yields all stabilise to the same value, 10 – 12g/g. This aligns with the same MLR seen for the oxidation period, with all values in the same range. At the end of the experiments the CO yield analysis become erratic with large fluctuations. This is due to the mass gain in the sample due to moisture within the air.

To allow for comparison across the experiments and the effect of the variation in exposure heat flux, the two described semi-steady state regions have been averaged, providing an averaged MLR for the assumed oxidation and pyrolysis phase and another for the oxidation only phase. The range utilised for the pyrolysis and oxidation region was based on when the rate of change over 1 minute exceeding 3%. This gave allowance to minor fluctuations, while still capturing the significant changes in rate of growth/decay. These averaged MLRs are plotted on Figure 24 against the initial exposure heat flux and do not represent the MLR of the sample when subjected to said heat flux.

For experiments 4, 8, 9 and 10 the determination of the steady state pyrolysis MLR was easily identifiable. However, experiment 7 showed signs of three minor plateaus within the expected range. Therefore, the resultant rate was established for the minor stabilised periods, with a weighted average of all 3 taken. The MLR for the oxidation phase, was clearly identifiable on all experiments.

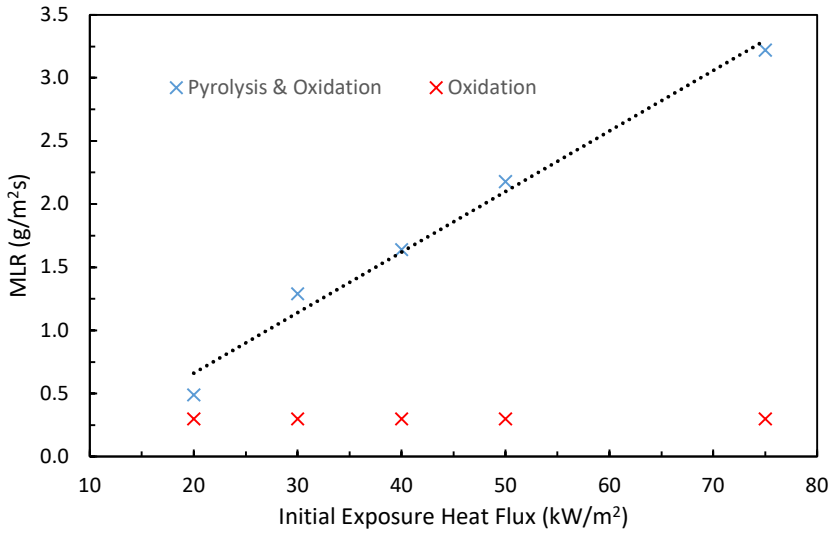

Figure 24: Averaged MLR for the pyrolysis and oxidation phase and oxidation phase

As shown on Figure 24, the higher the exposure heat flux, the higher the MLR during the steady state smouldering for the described pyrolysis and oxidation phase. There is an increasing linear relationship between the heat flux and MLR. However, as the heat flux increased, the duration of this steady state MLR reduced, which can be seen on Figure 22.

All experiments were exposed for approximately 15 minutes post ignition, except experiment 10 which was 19 minutes. Hence, over this time period the higher heat fluxes would be able to transfer more energy into the timber sample, regardless of the variation in ignition times. Due to the greater rate of energy being transferred into the timber, it would have a higher surface temperature, resulting in quicker heat transfer through the sample and deeper thermal penetration. This will also create deeper and faster moving pyrolysis and oxidation fronts, created from the increased conductive heat transfer stemming from a greater difference in temperature. Thus, there will be less unreacted timber within the sample. Once the heat flux was removed, the samples exposed to the higher heat fluxes would have a higher temperature, still promoting the increased pyrolysis and oxidation front, resulting in the higher MLR. And as this pyrolysis front has a higher propagation rate, the time seen for the steady state is less, as the uninvolved timber will be pyrolysed the quickest.

The heat losses from the samples were all comparative to one another, due to the same sample build up, hence is not deemed to be a point of contention. However, it is worth mentioning that the plasterboard that underwent the higher heat fluxes would experience more thermal degradation, which could result in greater heat losses to the front, due to increased cracking. Also, when plasterboard is heated above $700^{O}C$, its thermal conductivity starts to increase above that at ambient temperatures (McLaggan et al., 2018). But as no thermocouples were adopted, the plasterboard temperatures cannot be evaluated for this effect.

Finally, as mentioned prior, there appears to be no influence on the MLR associated with the oxidation phases, due to the varied exposure heat fluxes. All the MLR were found to be $0.3g/m^2s \pm 0.003g/m^2s$.

4.4.3 Smouldering Duration and Mass Loss

Table 5 summarises the smouldering times after the heat flux was set to $0kW/m^2$ and mass loss during it for the experiments. The ignition times come from section 4.4.1 and are discussed there. The end time for the smouldering was based on two factors, as explained within section 3.4, the CO production and mass loss. However, as explained in section 4.1, many experiments witnessed mass gain towards the end, attributed to moisture gain from the atmosphere in the sample. Thus, the extinction time was determined when the CO production rate fell to 0g/s highlighting no smouldering, while taking account of drift observed within the analyser.

Table 5: Data set 2 experiment time events for smouldering and its mass loss

Experiment Ref	Heat Flux	Exposure Time (min)	Ignition Time (min)	Smouldering Time Post heat flux removal (min)	Mass loss post heat flux removal (g)	Sustained Smouldering
10	75	30	12	**230**	**90.2**	Yes
4	50	30	15	**267**	**103.2**	Yes
7	40	35	17	**302**	**100.2**	Yes
8	30	38	23	**322**	**114.6**	Yes
9	20	52	38	**369**	**103.1**	Yes

As shown in Table 5, smouldering was seen for a substantial amount of time for all experiments, with the least being 230 minutes, when exposed to the maximum heat flux, 75kW/m^2. While the longest smouldering time was 369 minutes when exposed to the lowest heat flux, 20kW/m^2.

This is attributed to the same reason discussed in section 4.4.2. The 75kW/m^2 was able to heat the timber sample to higher levels. Hence, once the heat flux was removed the timber had more energy and with all samples subjected to similar heat losses, due to uniform sample construction, a greater MLR was seen, resulting in quicker consumption of the fuel.

The smouldering times post heat flux removal, are all significantly greater than the unexposed sample from experiment 1, see section 4.5.3 and Table 6, with an increase of 127 - 265%. Additionally, the mass loss post heat flux is considerably greater, with an increase of 30-65%. Thus, it is concluded that all the experiments within data set 2 witnessed sustained smouldering.

From inspection of the remains after the experiment, minimal char was left, as shown in Figure 25, with mainly ash present. The small amounts of char that were present, were always situated around the screws. This was observed for all experiments in this data set, with the char no greater than 10mm [W] x 10mm [H] x 10mm [D] in size.

Due to this, the extinguishment of the smouldering has been determined to be caused by 2 factors. Firstly, heat losses due to the screws. The only char left was situated around the screws and failed to oxidise. It would have experienced greater heat losses due to the metallic material of the screws having a high thermal conductivity and essentially acting as a thermal sink, easily transferring energy away from the char. Secondly, fuel depletion. Aside from the char around the screws, no other char or unreacted timber was present, hence, it is considered that the fuel was depleted.

(a)

(b)

(c)

(d)

Figure 25: (a) Char remains on screw after experiment 7 (b) Ash remains within insulation pocket after experiment 8: (c) Char remains on screw after experiment 10: (d) Char remains on screw after experiment 7

4.4.4 Summary

The results presented within data set 2 indicate that the heat flux utilised for the exposure does have an impact on the observed smouldering, with all experiments sustaining smouldering.

As expected, the higher the heat flux, the faster the ignition time. This increase was not linear, but instead a -0.852 power provided the best fitting trend line.

Once ignited, the measured CO production rate and MLR lead to the characterisation of two regions. First, a pyrolysis and oxidation phase, which showed signs of steady state smouldering. The time of this steady state decreased as the heat flux increased. This was followed by a rapid decay and another steady state smouldering period, but this time classified as predominantly oxidation.

It was found that the greater the initial heat flux, the greater the MLR for the steady state smouldering observed for the pyrolysis and oxidation phase. This provided a linear relationship, with the 75kW/m^2 exposure heat flux resulting in 3.22g/m^2s, which reduced to 0.42g/m^2s for the 20kW/m^2. However, there appeared to be no influence on the MLR during the steady state oxidation phase, with all experiments stabilising at 0.3g/m^2s ±0.003g/m^2s.

The determined self-sustained smouldering times were all in excess of 230 minutes, with the maximum 369 minutes, which is the time at which experiment 6 was ceased prematurely. Again, the exposure heat flux impacted these, with the smouldering times increasing as the heat flux decreases. This is believed to be due to fuel depletion. Based on this and the mass loss within this period, it was deemed that all experiments sustained smouldering.

4.5 Data Set 3 – Varying Encapsulation Material

Table 6 states the experiments to be presented within this data set and their corresponding variables. The main variable was the encapsulation material.

Table 6: Experimental variables for test within data set 3

Experiment Ref	Encapsulating Material	Exposure Time (min)	Heat Flux (kW/m^2)
1	None	15	50
2	Mineral wool	20	50
3a	1 layer of plasterboard	20	50
3b	1 layer of plasterboard	20	50
4a	1 layer of plasterboard	30	50
4b	1 layer of plasterboard	30	50
5a	2 layers of plasterboard	75	50
5b	2 layers of plasterboard	75	50
6	3 layers of plasterboard	150	50

4.5.1 Ignition Time

For all samples, the timber ignited during the exposure time, therefore, Figure 26 and Figure 27 only present the CO production rate and MLR during this time for clarity. For unity, the ignition of the timber shall be based from the CO production rate, as explained in section 4.4.1, with the derived ignition times listed in Table 7.

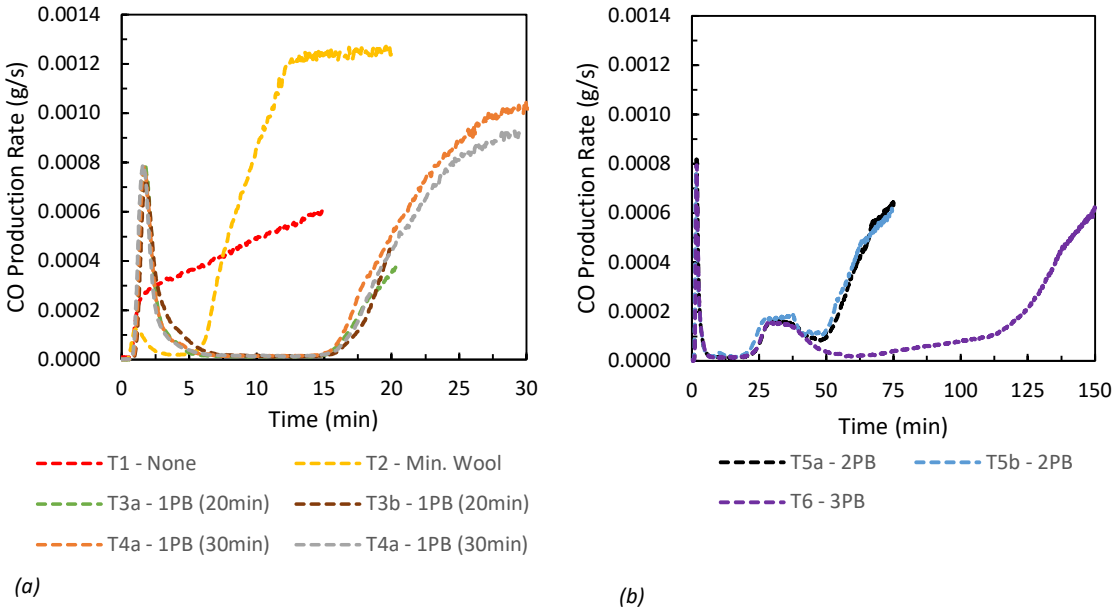

Figure 26: CO production rate for data set 3. (a) Experiments 1-4b: (b) Experiments 5a-6

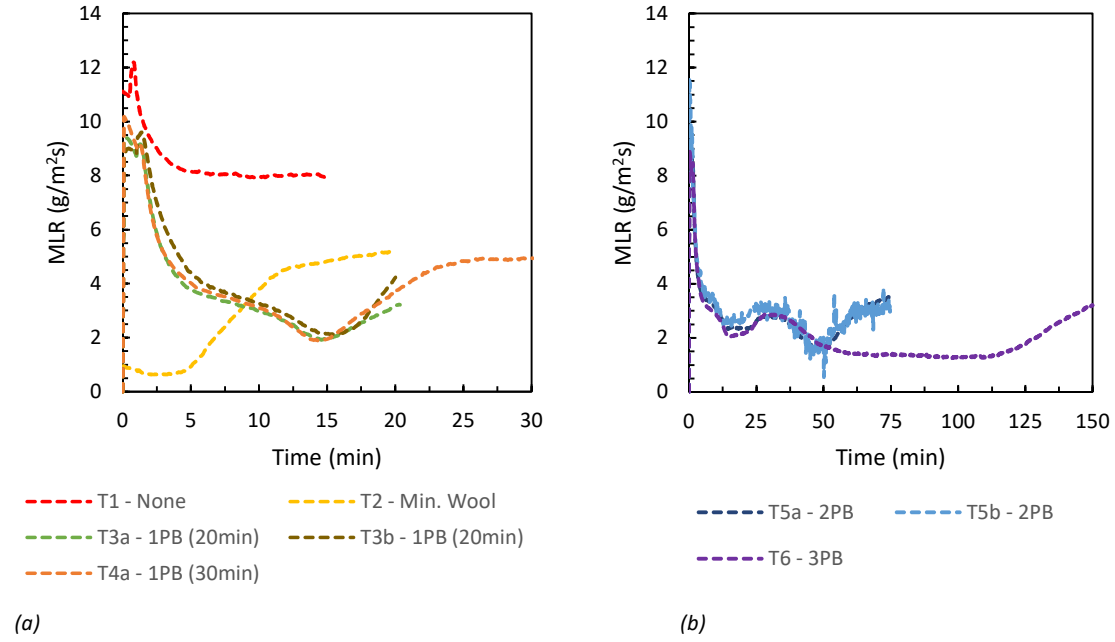

Figure 27: MLR for data set 3. (a) Experiments 1-4a: (b) Experiments 5a-6

The initial increase in CO rate seen in experiments 2 - 6 is caused by the encapsulating material and not the timber smouldering, confirmed from the findings in section 4.3. This is the same for the second increase and plateau observed at 20 – 50 minutes in experiments 5a, 5b and 6. However, for the triple layered plasterboard, experiment 6, the CO production after the second increase does not match that within section 4.3.

Table 7: Ignition times for data set 3

Experiment	Encapsulation Material	Ignition Time (min)
1	None	1
2	Mineral wool	6
3a	1 layer of plasterboard	17
3b	1 layer of plasterboard	17
4a	1 layer of plasterboard	16
4b	1 layer of plasterboard	17
5a	2 layers of plasterboard	49
5b	2 layers of plasterboard	50
6	3 layers of plasterboard	109

From inspection of Figure 26(b), experiment 6 CO production rate gradually increases from 63 minutes to 107 minutes linearly, where it to starts to increase at a greater rate. However, from the individual testing of three layers, a decay phase was seen after 92 minutes, which stabilised at 0.000022g/s, for the remainder of the experiment. Additionally, the MLR for experiment 6 exceeds that from section 4.3 within this time period, 0.01g/s compared to 0.0025g/s. This increased MLR could be a result of localised heating and pyrolysis in the timber, resulting from the metallic screws acting as a thermal bridge. Pyrolysis produces minor quantities of CO (Rein, 2009), hence, as this front spreads, the gradually increasing CO production rate from 63 minutes is seen. Once the plasterboard had been thermally penetrated and the timber face heated to pyrolysis temperature, the growth in MLR is seen, due to a much larger pyrolysis front. This is then followed by the sharp rise in CO production rate due to the oxidation of the char, which occurs at a later time due to a higher temperature needed. Despite all this, the ignition time has been determined as 109 minutes, due to the method explained in section 4.4.1.

Experiment 1 had the quickest ignition time of 1 minute. As there was no encapsulation to protect the timber, allowing for faster heat transfer. This is the only sample in which visible flaming was observed, occurring at 15 seconds.

Experiments 3a, 3b, 4a and 4b had the same encapsulation material, a single layer of plasterboard. This is reflected in Figure 26(a) and Figure 27(a), with their data lines overlaying with minor differences seen. This was the expected trend, with the consistency highlighting the repeatability and giving

confidence in uniform sample construction. This is also seen for the experiments with two layers of plasterboard, 5a and 5b.

Overall, the 25mm thick mineral wool provided the least encapsulation time at 5 minutes, followed by 1 layer of 12.5mm thick plasterboard at 15.5 minutes. As expected, the time to ignition was longer for the double and triple layer plasterboards, 48 - 50 minutes and 116 minutes respectively.

Even though the mineral wool was double the thickness, it provided less protection than the single layer plasterboard. From the manufacture data sheets (ETEX, 2019) (Rockwool, 2018), we know that the thermal conductivity, k, for the plasterboard is 5 times larger, at 0.19W/mK compared to 0.038W/mK, resulting in quicker energy transfer at the surface. The same can be said for the densities, with the plasterboard density 14 times greater, 640kg/m^3 compared to 45kg/m^3. From literature, we know that the two materials have specific heat capacities, c_p, in the same range, 950J/kgK for plasterboard (Mehaffey et al., 1994) and 850J/kgK for the mineral wool (Yousefi and Tariku, 2021).

Due to its significantly greater density, plasterboard is able to absorb greater amounts of energy before its temperature increases by 1K, even though it will absorb heat faster. This relationship can also be expressed as the thermal diffusivity of a material. The thermally diffusivity can be seen as the overall rate of heat transfer through a material and is given by equation (6):

$$\alpha = \frac{k}{\rho \cdot c_p} \tag{6}$$

The thermal diffusivity is calculated as 0.313mm/s and 0.994mm/s for the plasterboard and mineral wool respectively. As mineral wool has a higher value, it will allow for quicker heat transfer through its medium. Its value is more than double that of plasterboard and double the thickness, thus, results in quicker ignition times

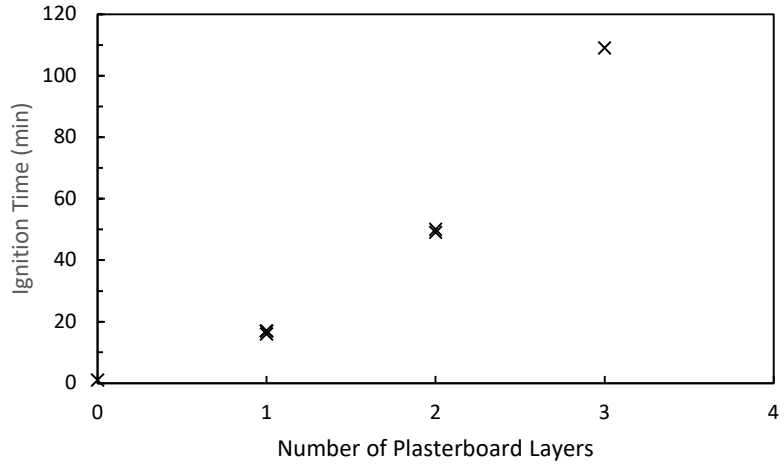

Figure 28: Ignition time plotted against varying number of plasterboard encapsulation layers

Figure 28 plots the ignition time for varying layers of plasterboard. As expected, with an increasing number of plasterboard layers, the time to ignition increases. All layers are the same thickness, hence there is a linear increase in the protection thickness, but a non-linear increase in ignition time is seen.

The interfaces between the plasterboard layers were subjected to heat losses. Due to minor imperfections on the surface of plasterboard, two layers won't be fully in contact, allowing ambient air to flow between. As this air becomes heated due to convection heat transfer, thermal buoyancy causes it to rise and be lost to the environment. Additionally, varying sizes of fissures were seen across the surface of the plasterboard, allowing for cooler ambient air to directly penetrate into the plasterboard layers, thus, increasing the heat losses. These fissures were a result of the thermal degradation of the plasterboard, hence, when the samples were exposed for a longer period of time, the outer layers developed more severe cracking. Consequently, the greater the number of plasterboard layers, the greater the heat losses.

This was reflected in experiment 6, which underwent severe thermal degradation during the heating phase. As described in section 4.1, the first layer of plasterboard fell forward creating a 0.5-3mm separation between the layers. At this separation the heat transfer method across would rely on convection. However, as the air in between was heated, it would be subjected to thermal buoyancy causing it to rise up, away from the sample. This led to increased heat losses and can be related to the increased ignition time.

4.5.2 Smouldering Characteristic

Figure 30 - Figure 36 present the CO production rate, CO yield and the MLR for the experiments, with the exposure time indicated with a dashed line. The initial peaks seen within the first 5 minutes for

the CO production and MLR are due to the encapsulation material reacting to the heat flux and is discussed in section 4.3 and 4.5.1, hence will not be included here.

Experiment 3a showed the shortest experimental time, due to its extinguishment. After the heat flux was removed, the CO production rate and MLR continued to rise for 4-5 minutes, before promptly decaying to zero. Refer to section 5.2 for further discussion.

Experiment 1, the unprotected timber, was the next shortest experiment. It provided the greatest increase in CO production rate, more than doubling once the heat flux was set to zero. The CO production showed the same trend of a double peak, with the maximum values within the same range, however this was not reflected by the MLR. Once the heat flux was removed, the MLR swiftly decayed. A minor growth period was observed between 26 – 31 minutes, from 3.82g/m^2s to 4.1g/m^2s. But again, after this the MLR continued to decay. A small stabilised region is observed at 75 -100 minutes, measured at 0.023g/m^2s ± -.002g/m^2s, which is associated with the oxidation region explained in section 4.4.2

The same trend discussed in section 4.4.2, was seen for the following experiments: 2, 3b, 4a and partially 4b. Only the CO production rate was recorded for experiment 4b, meaning no analysis on the MLR and CO yield can be given. However, based on the close alignment with experiment 4a, it is expected to provide similar values.

Experiments 5a, 5b and 6 showed similarities with that described in section 4.4.2 and still displayed signs of the two regions, a pyrolysis and oxidation phase and a mainly oxidation phase. The similarities arose in the MLR. The final spike at the point where the timber is stated as transitioning from thermally thick to thermally thin and the instantaneous decay afterwards to the stabilised MLR, which is assumed to be predominantly oxidation reactions. However, once the heat flux was turned off, the CO production rates continued to increase for a substantial amount of time, 24-35 minutes, compared to approximately 4 minutes for experiments 2-4. This resulted only in a single CO production rate peak, with a rapid decay to the final stabilised region. This longer growth was also observed for the MLR. Experiments 6 and 5b MLR continues to rise up to a small plateau, considered to be steady state smouldering. From this point onwards, the MLR follows that as discussed in section 4.4.2. However, there are major fluctuations seen on experiment 5b, which has been attributed to vibrational effects, due to a small part of the aluminium foil being in contact with the cone heater. However, the overall trends of growth and decay remain valid. If the data is expanded, a clear stabilised region can be seen for an extended period of time. Experiment 5a MLR continues to rise but then experiences a small decay phase, similar to that seen in experiments 2, 3b, 4a, but on a much smaller scale. From this point on it follows the MLR trend as discussed in section 4.4.2.

The CO yields for experiments 5a, 5b and 6 also differ to that of previous. Instead, a gradual increase is observed, to the time corresponding to the rapid decay observed for the MLR. At this point, a sharp rise in the yield is observed, which reverts back to a gradual increase. There appears to be no sign of a steady yield for the stabilised oxidation region, as seen within data set 2 and experiments 2 and 4a.

This observation is seen for the remaining experiments within this data set. The CO yields, never seem to stabilise, instead gradually increasing. All values are in the range of 0.125g/g, before major fluctuation are seen and become unreadable.

When comparing experiment 1, the exposed sample to the other experiments, it can be seen that the encapsulation has a major impact on the smouldering. Primarily due to the heat losses post heat flux removal, affecting radiative and convective losses. Firstly, as the char is oxidised, a void will form within the insulation pocket. With the presence of encapsulation, this can be seen to be a semi-sealed environment, helping to limit the flow of cool ambient air into this volume, coupled with the side insulation that too will hinder it. During the exposure this volume would become heated, increasing its temperature. Post heat flux removal, due to the limited flow, cold ambient air would not be as free to mix, reducing its temperature. Additionally, the encapsulation would help limit the effects of thermal buoyancy, helping to contain the hot gases within this volume, thus limiting heat losses to the environment. Secondly, the encapsulation surface will help reflect radiation back towards the reaction zones, helping to sustain the reactions.

This is reflected in the continuing decay in the MLR for experiment 1, without the reduced heat losses the MLR never appears to stabilise, except for the final oxidation region. Even then, this is only for approximately 50 minutes, compared to a minimum of 150 minutes for the remaining experiments.

The same method for determining an averaged MLR for the two regions as explained in section 4.4.2 is adopted, with the values for the pyrolysis and oxidation phase listed in Table 8. Again, these values represent the initial exposure heat flux and do not represent the MLR of the sample when subjected to said heat flux.

Table 8: Averaged MLR for pyrolysis and oxidation region

Experiment Ref	Encapsulating Material	Pyrolysis and Oxidation Phase - MLR (g/m^2s)
1	None	-
2	Mineral wool	2.93
3b	1 layer of plasterboard	2.00
4a	1 layer of plasterboard	2.19
5a	2 layers of plasterboard	3.29
5b	2 layers of plasterboard	3.66
6	3 layers of plasterboard	3.76

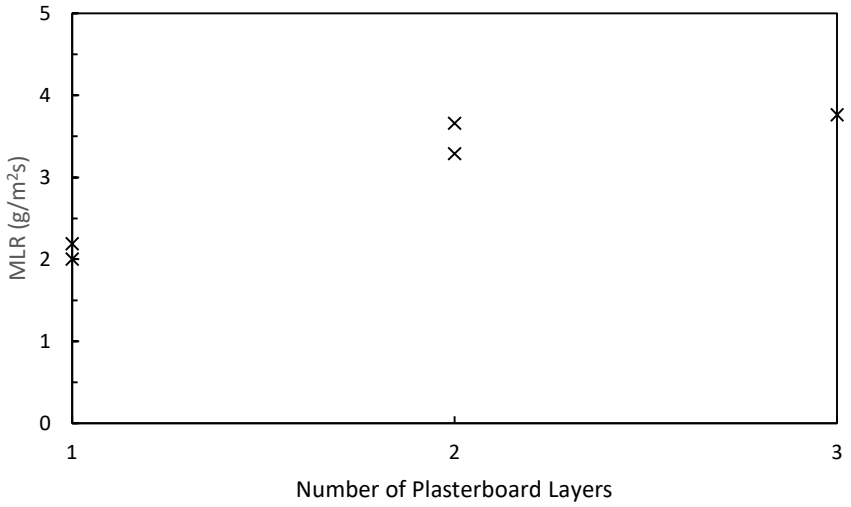

Figure 29: Averaged MLR for pyrolysis and oxidation period for varying layers of plasterboard

The different encapsulation buildups affected the observed smouldering dynamics. The triple layered plasterboard resulted in the greatest MLR observed for the pyrolysis and oxidation phase. This MLR decreased with plasterboard layers, but no apparent trend is visible, as shown on Figure 29. Due to the greater mass and thickness attributed with an increased number of plasterboard layers, they will be able to absorb and hold greater amounts of energy. This would require longer time for the heat to

dissipate to the environment. Thus, a smaller temperature difference would be seen at the rear of the plasterboard over a standardised time period, resulting in smaller conductive heat losses.

It was expected that the mineral wool would allow for greater oxygen transport through its medium, in turn leading to an increased MLR within the oxidation phase. However, this was not seen, with all encapsulation materials converging at the same rate MLR 0.30g/m^2s ±0.02g/m^2s. It should be noted that the sample insulation is constructed from the same mineral wool. Therefore, it is concluded that this provided an ample supply of oxygen to facilitate the maximum oxidation reaction.

Single layer plasterboard was tested with 20 and 30 minutes exposure time, which can be seen on Figure 32, Figure 33 and Figure 36. Omitting experiments 3a, which extinguished after heat flux removal, the experiments showed alignment. The peak values seen for the CO production rate and MLR are of the same range, with a time delay of 7-13 minutes for the decay phases. This is expected, due to the presence of the external heat flux for longer.

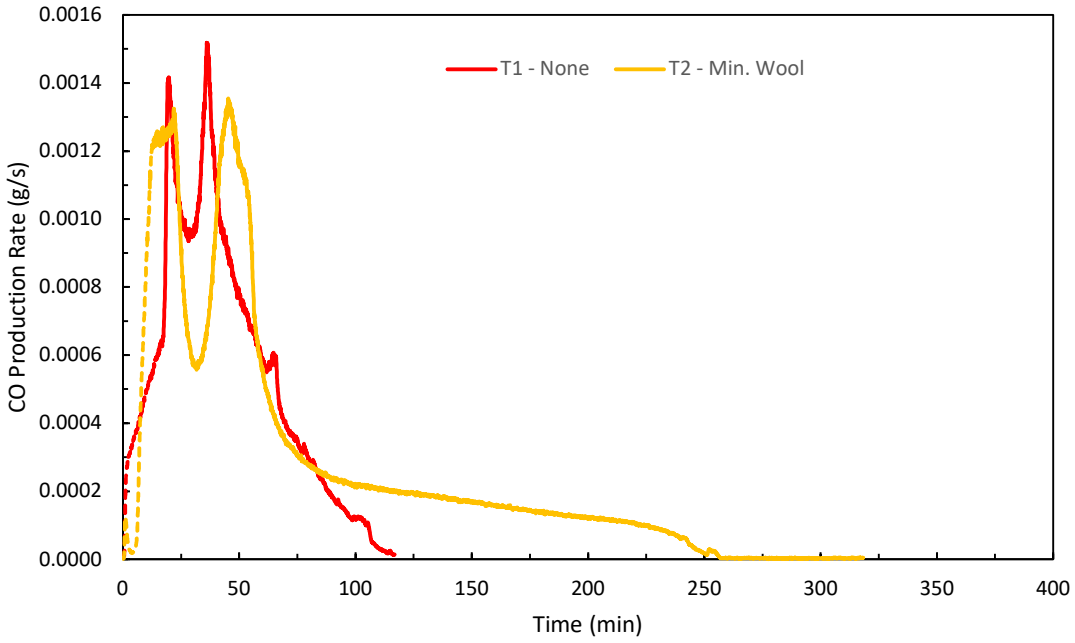

Figure 30: Experiments 1 and 2 CO production rate

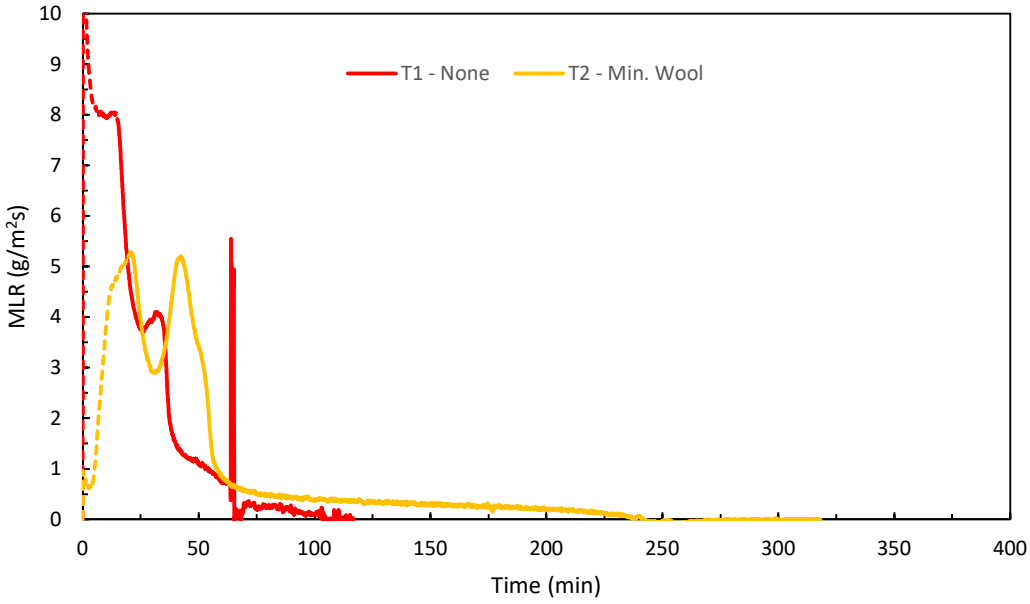

Figure 31: Experiments 1 and 2 MLR

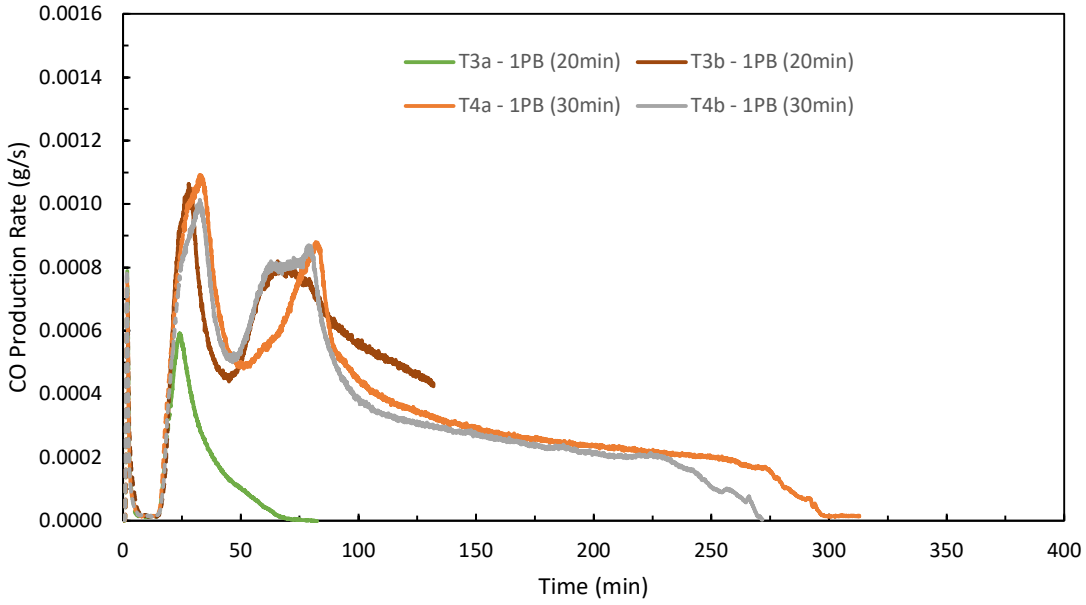

Figure 32: Experiments 3a, 3b, 4a and 4b CO production rate

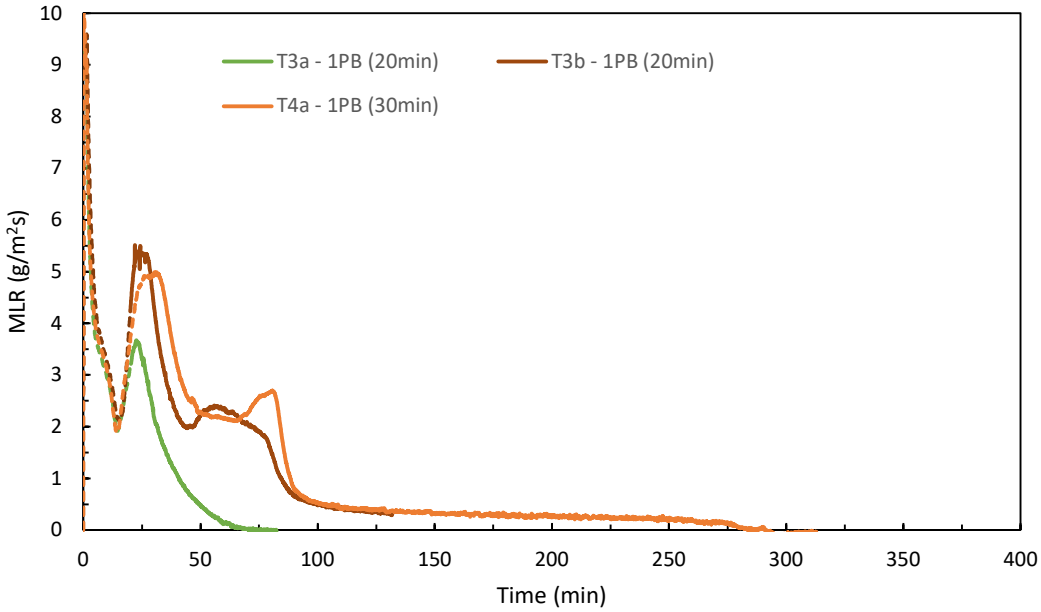

Figure 33: Experiments 3a, 3b, 4a and 4b MLR

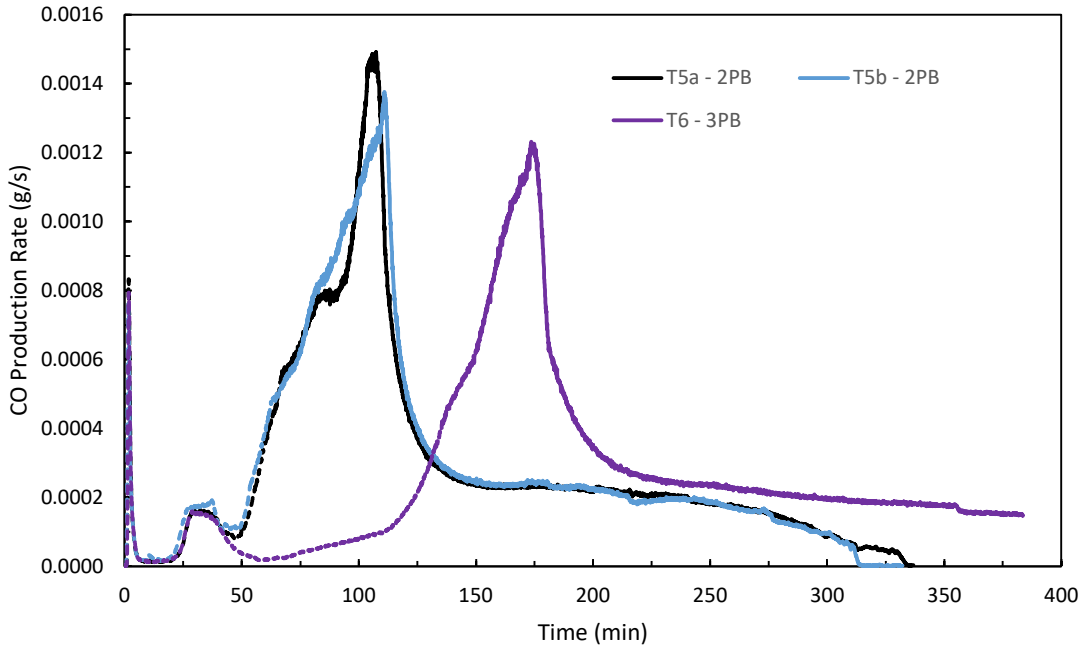

Figure 34: Experiments 5a, 5b and 6 CO production rate

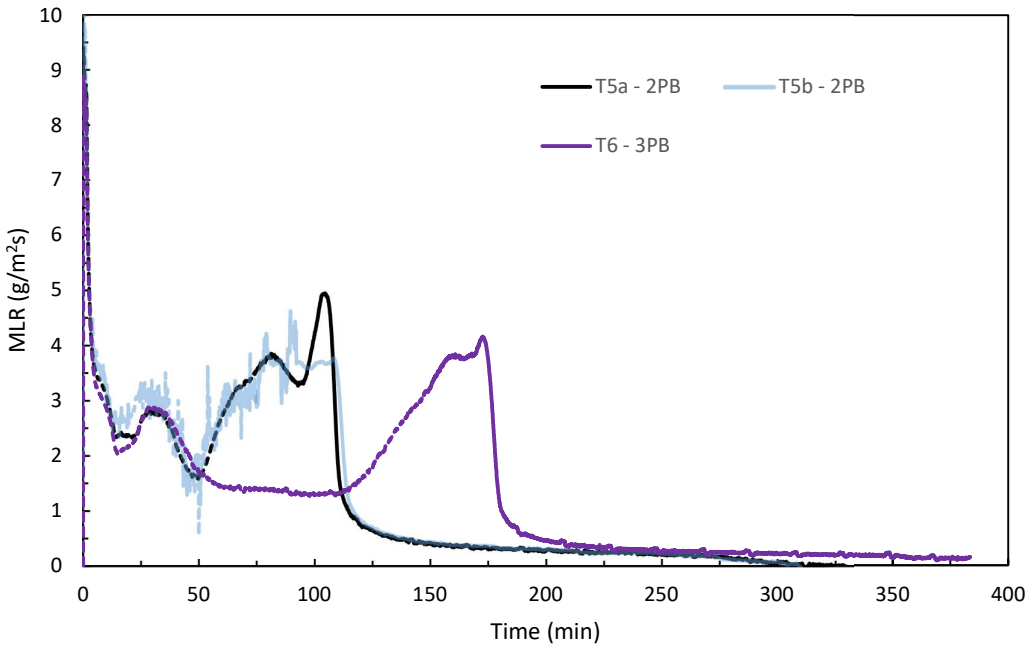

Figure 35: Experiments 5a, 5b and 6 MLR

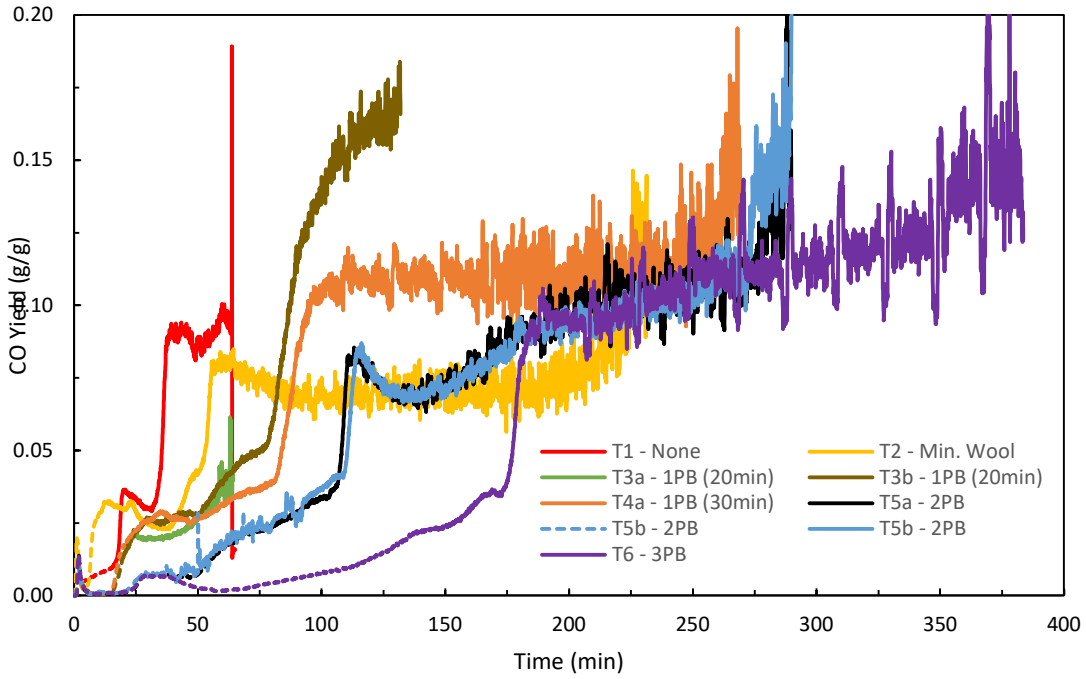

Figure 36: CO yield for experiments within data set 3

4.5.3 Smouldering Duration and Extinguishment

Table 9 summarises the smouldering times after the heat flux was set to 0kW/m^2 and mass loss during it for the experiments. The ignition times come from section 4.5.1 and are discussed there. The criteria for smouldering extinguishment are the same as described within section 4.4.3.

The smouldering time for experiment 1 was 101 minutes with a mass loss of 69.4g. Due to the rapid decay and short smouldering time post heat flux removal, it was deemed not to have sustained smouldering. Additionally, large sections of charred timber were observed after the experiment within the insulation wrapping. Due to the exposed face, there would have been considerable heat losses from the timber sample. This is considered to be the main reason that the smouldering extinguished and is discussed in section 4.5.2. However, from previous research results for exposed sections (Li, 2022) and the fact that slabs of timber cannot burn without an external heat flux (Drysdale, 2011), it was expected that the sample would extinguish much more quickly than observed.

Due to the complex nature of smouldering, there are various possible reasons why the sample smouldered longer than expected. This could be a result of the vertical cut, creating a radiative feedback system, providing the additional external heat flux as shown in equation (5) that is required for burning of timber. This would align with the large scale compartment testing, with CLT panel joints self-sustaining smouldering (Su et al., 2018a) (Wiesner et al., 2021) (Kotsovinos et al., 2023).

Table 9: Data set 3 experiment time events for smouldering and its mass loss

Experiment Ref	Encapsulating Material	Exposure Time (min)	Ignition Time (min)	Smouldering Time Post HF removal (min)	Mass loss post HF (g)	Sustained Smouldering
1	None	15	0.5	**101**	**69.4**	No
2	Mineral wool	20	6	**234**	**94.4**	Yes
3a	1 layer of plasterboard	20	17	**46**	**27.6**	No
3b	1 layer of plasterboard	20	17	**N/A**	**N/a**	N/A
4a	1 layer of plasterboard	30	16	**267**	**103.2**	Yes
4b	1 layer of plasterboard	30	17	**N/A**	**N/A**	Yes
5a	2 layers of plasterboard	75	49	**258**	**95.2**	Yes
5b	2 layers of plasterboard	75	50	**238**	**97.3**	Yes
6	3 layers of plasterboard	150	109	**>233**	**>79**	Yes

Alternatively, the exposure time may have been excessive, significantly increasing the sample's temperature, giving rise to deep thermal penetration and pyrolysis front, resulting in a comparatively thick char layer to the exposed face. This char would insulate the front face and in turn, limit the heat loss within equation (2). This would elongate the smouldering time. However, we can't be certain as to which, and it is most likely a combination of both these and other factors.

As experiment 1 had no encapsulation with exposed timber and is deemed not to have sustained smouldering, the other experiments shall be evaluated against it to establish if sustained smouldering was present.

Experiment 3a experienced the shortest smouldering time at 46 minutes and the least mass loss, 27.6g. This is drastically less than experiment 1, and therefore, deemed not to have sustained

smouldering. From visual inspection of the sample, the majority of the timber was unreacted. Further discussion is given in section 5.2.

Due to apparatus error, experiment 3b was ended prematurely. There is not enough data to accurately state that smouldering would have been sustained. However, based on the observed results, the CO production and MLR was noticeably greater relative to the other experiments in the decay phase. Consequently, we have a high degree of confidence that smouldering would have continued for an extended period of time.

Experiments 2, 4a, 4b, 5a, 5b and 6 all experienced extended smouldering times, in excess of 230 minutes, with a mass loss in the region of 100g during this time. Experiment 6 only recorded a mass loss of 79g. However as mentioned in section 4.1, the experiment was terminated when smouldering was still present. Based on the previous findings, it is deemed that smouldering would have continued for longer, resulting in an increased mass loss. Also, due to user error, no mass data was recorded for experiment 4b. When evaluated against experiment 1, the smouldering times were substantially greater with an increase of at 131 - 165% and an increase in the mass loss of 36 - 48% (excluding experiment 6 and 4b). Based on this, it is deemed that all these experiments sustained smouldering.

From inspection of the remains after experiments 2, 3b, 4a, 4b, 5a, 5b and 6, minimal char was left as shown in Figure 37(a)-(d), with mainly ash present. The small amounts of char present were situated around the screws, and all less than 10mm [W] x 10mm [H] x 10mm [D] in size. Due to this, the extinguishment of the smouldering has been determined to be caused by 2 factors, heat losses at the screws and fuel depletion, the same as section 4.4.3.

(a) *(b)* *(c)*

Figure 37: (a) Char remains on screw after experiment 4a and ash (b) Ash remains within insulation pocket after experiment 5a: (c) Char remains on screw after experiment 5b

4.5.4 Summary

From the experiments completed in data set 3, we have shown that the chosen encapsulation material and thickness does influence the smouldering characteristics. From the testing, all but 2 samples resulted in self-sustained smouldering. Experiment 3a, with a single layer of plasterboard and experiment 1, which had no encapsulation are the only two that did. However, other experiments with a single layer of plasterboard did lead to smouldering.

Omitting experiment 1, the mineral wool had the quickest ignition time, due to having the highest thermal diffusivity. The single layer plasterboard was the next quickest to ignite, with the ignition times increasing as the number of layers increased.

As discussed in data set 2, the data showed signs of the 2 varying regions again. From the various arrangements tested, it was found that the 3 layers of plasterboard resulted in the greatest MLR for the pyrolysis and oxidation region, with this reducing with the number of plasterboard layers. Apart from the reducing trend, no specific relationship was established. The final stabilised MLR associated with the oxidation phases was found to be 0.3g/m^2s ±0.003g/m^2s.

5 Further Discussion

5.1 Limitations and Uncertainties

The experimental testing and analysis were subjected to uncertainties and error.

As discussed, the gas analyser for the CO_2 and O_2 appeared faulty providing unreliable results. Therefore, this data was not used. This limited the analyses that could be completed, resulting in no HRR calculations and comparison of the CO_2 to the CO production.

Due to the faulty apparatus, the accuracy of the CO analyser has to be considered. The CO data displayed expected trends, reinforced with the measured mass loss that was independent from the analyser. Therefore, we are confident that the analysed data is reliable. Additionally, all testing was completed on the same apparatus, within a relatively short time frame, hence, there was uniformity across all experiments. If there was an underlying error with the analyser, this would be present on all experiments and the observed trends would still be valid.

The gas analysers were calibrated before every experiment, however, due to the long experimental times they are prone to drift. This was observed for numerous experiments, resulting in uncertainty of the values recorded during the experiment. The drift could easily be accounted for at the end of the experiment, but the time at which it started to occur is unknown. Albeit, the observed drift was minimal, and is believed to have minimal impact on the results, with a maximum effect of 1.1% on the peak values.

The heat flux to the sample surface was impacted by numerous factors. Firstly, ambient conditions in the lab. As the exposure time was up to 150 minutes, changes in the laboratory temperature would impact the final heat flux. This is believed to have minor effect on the overall results. Secondly, the positioning of the sample holder. Care was taken to ensure almost uniform positioning of the sample holder to provide 25mm standoff. However, due to the speed required in placing the sample to limit exposure before the mass could be measured, ensuring exactly the same positioning each time was unfeasible. Finally, the samples were positioned vertically, but during the experiment certain samples rotated forward marginally, reducing the 25mm standoff. These factors would lead to an uneven heat flux to the sample surface.

The recorded data was prone to minor fluctuations, due to the nature of the experiments. Therefore, it was difficult to determine precise timing of events, with regard to the ignition and extinguishment of the timber. Consequently, the determined times may be inaccurate, however, we are confident that all times are within ±1 minute.

No thermocouples or imaging technology was utilised. Due to this, temperature profiles of the samples could not be determined.

Finally, the boundary conditions. The selected side and read insulation of 30mm was solely based from previous research (Li, 2022). However, the extent of their effect has not been quantified, therefore, we do not know the effect a variation in these conditions will have on the results.

5.1.1 Repeatability

Due to the considerable time requirements for each experiment, coupled with the time constraints of the project, minimal repeats were completed. Thus, only three experiments were repeated, 3b, 4b and 5b, of which data logging issues were seen for experiment 4b.

As shown in section 4.5, experiments 4b and 5b, very closely aligned with the results of experiment 4a and 5a. The measured data was typically within 5% of the corresponding experiment. The only major difference seen was the time for the CO production rate to fall to 0g/s for experiments 4a and 4b, where the difference was 10%.

Due to the swift extinguishment of experiment 3a, while 3b continued to smoulder, the results cannot be said to align.

5.2 Experiment 3a – Observed Smouldering and Its Extinguishment

As shown in section 4.5, experiment 3a quickly extinguished and did not sustain smouldering, see Figure 38(a) and (b) for the remains.

The top of the sample showed greater extents of pyrolysis with more char present and a reduction in its dimensions. At the bottom edge, the timber remained predominantly unreacted. From the side view, the pyrolysis depth can be seen to be increasing with height, with same observations seen to the inside of the cut.

This highlights the effect of the vertical orientation on the smouldering dynamics, since the surface was heated as evenly as possible, but more evidence of smoulder was observed at the top. The airflow over vertical samples varies to that over horizontal, as thermal buoyancy drives upwards airflow over the sample surface, promoting an increased convective heat transfer (Bartlett et al., 2019). Thus, the heat transfer will increase as height increases, which is reflected from the deeper pyrolysis front and char. However, whether this would result in an increased MLR over horizontal samples is unknown, with contradicting evidence seen from previous research into orientation (Bartlett et al., 2019)

Experiment 3b had the same variables as 3a, but displayed very different results, see Figure 32 and Figure 33. As discussed, 3b showed signs of sustaining smouldering, but the experiment was prematurely ended. This could cast doubt about the repeatability of these experiments. Additionally, we have seen from section 4.5, experiments 4a and 4b, which had the same sample construction but 10 minutes longer exposure time, that this additional time did affect the smouldering, due to differing results. This raises the question as to whether there is a critical exposure time required post ignition in order for smouldering to sustain. Experiments 3a and 3b were exposed to the heat flux for 3 minutes after ignition, compared to 13-14 minutes for experiments 4a and 4b. Furthermore, there would be minor imperfections and differences between the samples, which would result in fractionally different heating regimes. If this critical exposure time post ignition is around 3 minutes, this could be the difference between the extinguishment or sustained smouldering of the sample. However, as no other repeats were completed, no definitive conclusion can be made.

(a) *(b)*

Figure 38: Remains from experiment 3a highlighting the char pattern. (a) Front view: (b) View of the sides

5.3 Long Ignition Time – Is Sustained Smouldering a Hazard?

The time to ignition for the triple layered plasterboard was established as 109 minutes for 50kW/m^2, well beyond the duration of a typical compartment fire duration. This raises the question as to whether self-sustained smouldering would be an issue for triple layered plasterboard or greater protection for higher heat fluxes. From a theoretical view point, with ideal conditions, we would expect this level of protection to mitigate this hazard. However, in practice this is not the case.

A common occurrence seen within large scale testing and real-life fires is plasterboard fall off when subjected to fire. This occurs due to degradation of the plasterboard, with cracks and fissures forming and the integrity of the plasterboard reducing (Rahmanian, 2011). Additionally, due to this, the screws can be pulled though the boarding, leading to failure.

Once the plasterboard falls off, increased heat transfer would occur to the substrata. Various research has been conducted in an attempt to quantify the temperatures at which it occurs. But due to the complex nature of plasterboard's thermal response and deterioration, no fixed temperature has been established (Sultan, 2008) (Rahmanian, 2011).

The plasterboards within our experiments were essentially self-supporting, bearing their own weight along their bottom edge and not relying on the screwed fixings for stability. No plasterboard fall off or full collapse was witnessed during the testing, but experiment 6 showed signs that a collapse was fast approaching if heating continued, see Figure 12. Cracking and fissures were seen for all experiments, with the longer exposure times and higher heat fluxes showed signs of more intense deterioration. Also, as described in section 4.1, the majority of the fissures appeared to stem from the screw locations or to pass through them, highlighting that the screw holes created a weak point within the board, leading to the path of least resistance and helping to facilitate the cracking. However, the screw spacing within our samples was considerably less than industry standards.

It is therefore deemed, that due to practical application and issues coupled with the thermal degradation of plasterboard, adopting an increasing number of plasterboard layers until the ignition time is excessive is not suitable in mitigating this hazard.

5.4 Was The Cut Beneficial?

From the apparatus set up and data analysis, the effect of the cuts on the smouldering cannot be determined. However, the objectives of the research were not to establish how the cut would affect the fire dynamics, instead, the cut was present to help create conditions that were favourable to sustain smouldering based on previous experimental testing (Su et al., 2018a) (Wiesner et al., 2021) (Kotsovinos et al., 2023).

With that being said, based on the smouldering time post heat flux removal for the unexposed sample, experiment 1, which continued for 101 minutes, it is believed to have had a positive effect.

As seen, the encapsulated samples continued to smoulder, leaving minimal residual char sections. At some point during the experiments, any positive effect from the cut would become non-existent. This would be brought about by the distance between the two faces becoming excessive and overcoming the feedback system or by the timber being fully consumed to one side of the cut.

To allow for analysis of the cut's effect, future testing should incorporate imaging technology to help map the temperature profiles at the cut and how this develops.

5.5 Large Scale vs Small Scale Testing

Self-sustained smouldering has been observed on numerous occasions within large scale experiments, mainly compartment fires. But with the limited small-scale testing completed to date, replicating these conditions has been troublesome (Li, 2022). This can be attributed to the following:

Rein (Rein, 2009) proposed that samples' heat losses are proportional to the surface area, while the heat generated from oxidation is proportional to the volume. Hence, the smaller a sample becomes, the greater the surface area to volume ratio becomes, increasing the effect of heat losses. This has been used to provide a critical sample size, with smouldering unable to sustain itself without external interference. Therefore, for small scale testing the heat losses are deemed to have a greater influence.

The majority of the testing within this report and prior (Li, 2022) was completed with a maximum heat flux of 50kW/m^2. Actual room fires could easily be subjected to more extreme heat fluxes, with 200kW/m^2 observed within certain large-scale experiments (Veloo and Quintiere, 2013). This would have a direct impact on the observed smouldering dynamics, with greater heat transfer to the timber.

The testing of small-scale samples is subjected to additional heat losses through their sides, although this has been reduced via insulation, it is not zero. If these samples were theoretically merged into a larger wall panel within a compartment fire, it would not exhibit heat losses at the side, instead energy would be transferred within the timber, propagating the smouldering fronts. When considering an entire panel, standard construction methods would have timber panels abutting each other, limiting the heat losses at its side.

Finally, consider a compartment fire, post flaming extinguishment, but while smouldering is still present. Part of the heat from the smouldering would be lost to the air within the compartment, increasing its temperature. This in turn, would reduce the temperature difference between the compartment boundaries and the air, resulting in lower heat losses.

6 Conclusion

The experimental work completed within this report, sought to build on from previous work completed by Li (Li, 2022), looking into the impact of varying exposure heat flux and encapsulation build up for vertical samples.

From the experimental testing, nearly all the testing resulted sustained smouldering, with swift extinguishment observed for a single layer of player board when exposed to 50kW/m^2. However, when this was repeated, and during other experiments with one layer of plasterboard, sustained smouldering was observed.

It was found that the exposure heat flux has a direct impact on the smouldering dynamics, with a higher heat flux resulting in a greater MLR associated with a pyrolysis and oxidation phase. There is a linear relationship between the exposure heat flux and this MLR. Once this decayed, a final steady state MLR was observed, associated with being primarily oxidation. This was unaffected from the initial heat flux with all experiments experiencing the same. The heat flux had an impact on the observed smouldering times, with the higher initial heat fluxes resulting in shorter duration. This was due to the quicker consumption of the fuel.

The chosen encapsulation material influences the dynamics as well. As the experiments utilised the same side and rear insulation, the variations in the results within data set 3 are consequently due to the encapsulation material. It was found that triple layered plasterboard resulted in the greatest MLR compared to the single and double layers.

The triple layered plasterboard delayed the onset of smouldering by 109 minutes, giving confidence in its fire protection properties. However solely relying on this extended ignition delay time is not a suitable method for mitigating this hazard, due to the significant thermal degradation the plasterboard undergoes, hence its integrity cannot be guaranteed.

Previous small-scale research was not successful in creating conditions for sustained smouldering with plasterboard encapsulation. However, that was not the situation here, with all but 1 experiment self-sustaining smouldering. Coupled with the fact that large scale testing has alsoobserved self-sustained smouldering, major concerns need to be raised within the industry.

The building of high-rise structure with timber is seriously impacted due to the fire safety concerns associated with it, therefore, providing a solid foundation of knowledge is of the utmost importance, in which this research will play its role.

6.1 Future Works

To help, aid and further the field's knowledge related to this phenomenon, more experimental research is required. Due to the limited research specifically aimed at this problem, there is a wide array of conditions that could be tested. However, we believe the following testing would be most advantageous:

- Additional repeats for the completed experiments within this report, to provide confidence on the repeatability and reliability of the findings. At the same time, more detailed analysis can be completed with a working CO_2 and O_2 analyser.
- Experimental testing aimed at decoupling the pyrolysis and oxidation reaction to establish MLR for each.
- Testing with thicker timber samples. As discussed, samples showed signs of steady state smouldering, but it is believed the timber fully pyrolysed, resulting in the rapid decay of MLR before stabilising at around 0.3g/m^2s, while the charred timber oxidised. Testing with thicker samples will help investigate this steady state, whether the conditions would facilitate the increased MLR seen.
- Testing with samples orientated horizontally, but thermally exposed from below. This would help replicate conditions found on compartment ceilings.

The overall aim of research into this topic should be framed within the goal of establishing conditions that lead to sustained smouldering and quantifying their effect on the smouldering dynamics, mainly the MLR and charring rates. This is to provide the industry with confidence moving forward for the adoption of timber. If as seen, conditions prove to have adverse effect, the conversation needs to be had within the industry, design and regulatory bodies alike, about how to incorporate this into the structural design of timber members.

7 References

Babrauskas, V., 1984. Development of the cone calorimeter?A bench-scale heat release rate apparatus based on oxygen consumption. Fire Mater. 8, 81–95. https://doi.org/10.1002/fam.810080206

Bartlett, A., Wiesner, F., Hadden, R., Bisby, L., Lane, B., Lawrence, A., Palma, P., Frangi, A., n.d. NEEDS FOR TOTAL FIRE ENGINEERING OF MASS TIMBER BUILDINGS.

Bartlett, A.I., Hadden, R.M., Bisby, L.A., 2019. A Review of Factors Affecting the Burning Behaviour of Wood for Application to Tall Timber Construction. Fire Technol. 55, 1–49. https://doi.org/10.1007/s10694-018-0787-y

Bijloos, M., Lougheed, G.D., Su, J.Z., Bénichou, N., 2014. Solutions for mid-rise wood construction: cone calorimeter results for encapsulation materials: report to Research Consortium for Wood and Wood-Hybrid Mid-Rise Buildings. National Research Council of Canada. https://doi.org/10.4224/21274567

BSI, 2020. BS ISO 5660-1:2015+A1:2019. Reaction-to-fire tests. Heat release, smoke production and mass loss rate Heat release rate (cone calorimeter method) and smoke production rate (dynamic measurement).

BSI, 2004. BS EN 520:2004 Gypsum plasterboards - Definitions, requirements and test methods (+A1:2009).

BSI, 1995. BS EN 1995-1-1:2004+A2:2014. Eurocode 5: Design of timber structures - General Common rules and rules for buildings.

Buchanan, A., Östman, B., Tratek, S., Frangi, A., 2014. FIRE RESISTANCE OF TIMBER STRUCTURES.

Change, N.G.C., 2023. Carbon Dioxide Concentration | NASA Global Climate Change [WWW Document]. Clim. Change Vital Signs Planet. URL https://climate.nasa.gov/vital-signs/carbon-dioxide (accessed 5.5.23).

Chorlton, B., Gales, J., 2020. Fire performance of heritage and contemporary timber encapsulation materials | Elsevier Enhanced Reader [WWW Document]. https://doi.org/10.1016/j.jobe.2020.101181

Committee on Climate Change, 2019. UK housing: Fit for the future? London.

Crielaard, R., Van De Kuilen, J.-W., Terwel, K., Ravenshorst, G., Steenbakkers, P., 2019. Self-extinguishment of cross-laminated timber. Fire Saf. J. 105, 244–260. https://doi.org/10.1016/j.firesaf.2019.01.008

Dietenberger, M.A., Hasburgh, L.E., 2016. Wood Products: Thermal Degradation and Fire, in: Reference Module in Materials Science and Materials Engineering. Elsevier, p. B9780128035818033000. https://doi.org/10.1016/B978-0-12-803581-8.03338-5

Drysdale, D., 2011. An Introduction to Fire Dynamics.

ETEX, 2019. Technical Data Sheet - GTEC Standard Board.

Fangrat, J., Hasemi, Y., Yoshida, M., Hirata, T., 1996. Surface temperature at ignition of wooden based slabs. Fire Saf. J. 27, 249–259. https://doi.org/10.1016/S0379-7112(96)00046-X

Foster, R., Ramage, M., Reynolds, T., 2017. Rethinking CTBUH Height Criteria In the Contect of Tall Timber. CTBUH J. 2017, 28–33.

Friquin, K.L., 2011. Material properties and external factors influencing the charring rate of solid wood and glue-laminated timber. Fire Mater. 35, 303–327. https://doi.org/10.1002/fam.1055

Ghazi Wakili, K., Koebel, M., Glaettli, T., Hofer, M., 2015. Thermal conductivity of gypsum boards beyond dehydration temperature: THERMAL CONDUCTIVITY OF GYPSUM BOARDS. Fire Mater. 39, 85–94. https://doi.org/10.1002/fam.2234

Hasburgh, L., 2016. Fire Performance of Mass-Timber Encapsulation Methods and the Effect of Encapsulation on Char Rate of Cross-Laminated Timber.

Janssens, M. (n.d.). Calorimetry. In M. J. Hurley (Ed.), SFPE Handbook of Fire Protection Engineering (5th Edition ed., pp. 905-951). Springer.

Karacabeyli, E., Lum, C., 2022. Technical Guide for the Design and Construction of Tall Wood Buildings in Canada (No. SP-543E). FPInnovations, Pointe-Claire.

Kotsovinos, P., Christensen, E.G., Glew, A., O'Loughlin, E., Mitchell, H., Amin, R., Robert, F., Heidari, M., Barber, D., Rein, G., Schulz, J., 2023. Impact of partial encapsulation on the fire dynamics of an open-plan compartment with exposed timber ceiling and columns: CodeRed #04. Fire Mater. 47, 597–626. https://doi.org/10.1002/fam.3112

Li, H., 2022. Smoldering of Encapsulated Engineered Timber.

MacLeod, C.E., Law, A., Hadden, R.M., 2023. Quantifying the heat release from char oxidation in timber. Fire Saf. J. 138, 103793. https://doi.org/10.1016/j.firesaf.2023.103793

McLaggan, M.S., Hadden, R.M., Gillie, M., 2018. Fire Performance of Phase Change Material Enhanced Plasterboard. Fire Technol. 54, 117–134. https://doi.org/10.1007/s10694-017-0675-x

Mehaffey, J.R., Cuerrier, P., Carisse, G., 1994. A model for predicting heat transfer through gypsum-board/wood-stud walls exposed to fire. Fire Mater. 18, 297–305. https://doi.org/10.1002/fam.810180505

Mitchell, H., Kotsovinos, P., Richter, F., Thomson, D., Barber, D., Rein, G., 2023. Review of fire experiments in mass timber compartments: Current understanding, limitations, and research gaps. Fire Mater. 47, 415–432. https://doi.org/10.1002/fam.3121

Morrisset, D., Hadden, R.M., Bartlett, A.I., Law, A., Emberley, R., 2021. Time dependent contribution of char oxidation and flame heat feedback on the mass loss rate of timber. Fire Saf. J. 120, 103058. https://doi.org/10.1016/j.firesaf.2020.103058

Ohlemiller, T.J., 1985. MODELING OF SMOLDERING COMBUSTION PROPAGATION.

Östman, B., Brandon, D., Frantzich, H., 2017. Fire safety engineering in timber buildings. Fire Saf. J. 91, 11–20. https://doi.org/10.1016/j.firesaf.2017.05.002

Purser, D. (2002). Toxicity assessment of combustion products. In SFPE hand book of fire protection engineering 3

Rahmanian, I., 2011. Thermal and Mechanical Properties of Gypsum Boards and Their Influences on Fire Resistance of Gypsum Board Based Systems (Ph.D.). The University of Manchester (United Kingdom), England.

Ramage, M.H., Burridge, H., Busse-Wicher, M., Fereday, G., Reynolds, T., Shah, D.U., Wu, G., Yu, L., Fleming, P., Densley-Tingley, D., Allwood, J., Dupree, P., Linden, P.F., Scherman, O., 2017. The wood from the trees: The use of timber in construction. Renew. Sustain. Energy Rev. 68, 333–359. https://doi.org/10.1016/j.rser.2016.09.107

Ranger, L., Eng, P., Dagenais, C., Eng, P., Bénichou, N., 2020. ENCAPSULATION OF MASS TIMBER FLOOR SURFACES.

Rein, G., 2016. Smouldering Combustion, in: SFPE Handbook of Fire Protection. Springer, pp. 581–603.

Rein, G., 2013. Smouldering Fires and Natural Fuels, in: Belcher, C.M. (Ed.), Fire Phenomena and the Earth System. John Wiley & Sons, Oxford, pp. 15–33. https://doi.org/10.1002/9781118529539.ch2

Rein, G., 2009. Smouldering Combustion Phenomena in Science and Technology 1.

Richter, F., Jervis, F.X., Huang, X., Rein, G., 2021. Effect of oxygen on the burning rate of wood. Combust. Flame 234, 111591. https://doi.org/10.1016/j.combustflame.2021.111591

Rockwool, 2018. RW semi-rigid and rigid slabs.

Ronda, A., Della Zassa, M., Biasin, A., Martin-Lara, M.A., Canu, P., 2016. Experimental investigation on the smouldering of pine bark | Elsevier Enhanced bark. Fuel 193, 81–94. https://doi.org/10.1016/j.fuel.2016.12.028

Ronquillo, G., Hopkin, D., Spearpoint, M., 2021. Review of large-scale fire tests on cross-laminated timber. J. Fire Sci. 39, 327–369. https://doi.org/10.1177/07349041211034460

Su, J., Lafrance, P.-S., Hoehler, M., Bundy, M., 2018a. Fire Safety Challenges of Tall Wood Buildings - Phase 2: Task 2 & 3 - Cross Laminated Compartment Fire Tests. National Research Council of Canada.

Su, J., Leroux, P., Lafrance, P.-S., Gratton, K., Gibbs, E., Weinfurter, M., 2018b. FIRE TESTING OF ROOMS WITH EXPOSED WOOD SURFACES IN ENCAPSULATED MASS TIMBER CONSTRUCTION.

Sultan, M., 2008. Fall-off of gypsum plasterboard in fire.

Veloo, P.S., Quintiere, J.G., 2013. Convective heat transfer coefficient in compartment fires. J. Fire Sci. 31, 410–423. https://doi.org/10.1177/0734904113479001

White, R.H., Dietenberger, M.A., 2010. Fire Safety of Wood Construction, in: Wood Handbook, Wood as an Engineering Material.

Wiesner, F., 2019. Structural behaviour of cross-laminated timber elements in fires.

Wiesner, F., Bartlett, A., Mohaine, S., Robert, F., McNamee, R., Mindeguia, J.-C., Bisby, L., 2021. Structural Capacity of One-Way Spanning Large-Scale Cross-Laminated Timber Slabs in Standard and Natural Fires. Fire Technol. 57, 291–311. https://doi.org/10.1007/s10694-020-01003-y

Yousefi, Y., Tariku, F., 2021. Thermal Conductivity and Specific Heat Capacity of Insulation materials at Different Mean Temperatures. J. Phys. Conf. Ser. 2069, 012090. https://doi.org/10.1088/1742-6596/2069/1/012090

Zehfuß, J., Sander, L., 2021. Gypsum plasterboards under natural fire—Experimental investigations of thermal properties. Civ. Eng. Des. 3, 62–72. https://doi.org/10.1002/cend.202100002